Oxytocin receptor controls promiscuity and development in prairie voles

Ruchira Sharma[1,2,3,4†], Kristen M. Berendzen[1,2,3,4†], Amanda Everitt[1,3,10,11], Belinda Wang[1,3], Gina Williams[1,2,3,4,5], Shuyu Wang[1,2,3,4], Kara Quine[1,2,3,4], Rose D. Larios[1,2,3,4,5,14], Kimberly L. P. Long[1,2,3,4], Nerissa Hoglen[1,2,3,4,5], Bibi Alika Sulaman[1,2,3,4,15], Marie C. Heath[1,2,3,4,16], Michael Sherman[1,2,3,4], Robert Klinkel[1,2,3,4,17], Angela Cai[1,2,3,4,20], Denis Galo[1,2,3,4,], Lizandro Chan Caamal[1,2,3,4,18], Nastacia L. Goodwin[1,2,3,4,19], Annaliese Beery[6,7], Karen L. Bales[8,9], Katherine S. Pollard[10,11,12], Arthur Jeremy Willsey[1,13], Devanand S. Manoli[1,2,3,4,*]

[1]Department of Psychiatry and Behavioral Sciences

[2]Center for Integrative Neuroscience

[3]Weill Institute for Neurosciences

[4]Kavli Institute for Fundamental Neuroscience

[5]Neurosciences Graduate Program, University of California, San Francisco; San Francisco, CA 95158, USA

[6]Department of Integrative Biology

[7]Department of Neuroscience, UC Berkeley, Berkeley, CA, United States

[8]Department of Psychology

[9]Department of Neurobiology, Physiology, and Behavior, University of California, Davis; Davis, CA 95616, USA

[10]Gladstone Institutes, San Francisco, CA, USA

[11]Department of Epidemiology & Biostatistics, University of California, San Francisco, San Francisco, CA, USA

[12]Chan Zuckerberg Biohub, San Francisco, CA, USA

[13]Calico Labs, San Francisco, CA 94080, USA

[14]Neurona Therapeutics, South San Francisco, CA 94080, USA

[15]Department of Neuroscience, University of Michigan, Ann Arbor, MI 48109, USA

[16]Department of Neurobiology and Behavior, University of California, Irvine; Irvine, CA 92697, USA

[17]Branch Out School, Los Angeles, CA 90026, USA

[18]University of California, Los Angeles; Los Angeles, CA 90095, USA

[19]Department of Psychology, University of Washington; Seattle, WA 98195, USA

[20]Department of Rehabilitation and Regenerative Medicine, Columbia University Irving Medical Center; New York, NY 10032, USA

* Corresponding authors. Devanand.manoli@ucsf.edu

Lead Contact: Devanand.manoli@ucsf.edu

†These authors contributed equally to this work

Summary:

Oxytocin receptor (Oxtr) signaling influences complex social behaviors in diverse species, including social monogamy in prairie voles. How Oxtr regulates specific components of social attachment behaviors and the neural mechanisms mediating them remains unknown. Here, we examine prairie voles lacking Oxtr and demonstrate that pair bonding comprises distinct behavioral modules: the preference for a bonded partner, and the rejection of novel potential mates. Our longitudinal study of social attachment shows that Oxtr sex-specifically influences early interactions between novel partners facilitating the formation of partner preference. Additionally, Oxtr suppresses promiscuity towards novel potential mates following pair bonding, contributing to rejection. Oxtr function regulates coordinated patterns of gene expression in regions implicated in attachment behaviors and regulates the expression of oxytocin in the paraventricular nucleus of the hypothalamus, a principal source of oxytocin. Thus, Oxtr controls genetically separable components of pair bonding behaviors and coordinates development of the neural substrates of attachment.

Keywords:

Attachment behaviors, prairie vole, pair-bonding, oxytocin receptor, partner preference, monogamy, promiscuity, oxytocin signaling, paraventricular nucleus of the hypothalamus, nucleus accumbens

Introduction

Social attachments, such as the bonds between parents and children, family and kin, friends, and the long-term relationships between mates and romantic partners form the basis of interpersonal and group dynamics within societies[1–7]. Across mammals and other taxa, various selective pressures have given rise to diverse patterns of complex social organization involving long-term relationships between members of a species, one of the most robust and intriguing of which is the enduring bond between mates[2,4,8–13]. In mammals, ~4% of species demonstrate social monogamy, forming persistent pair bonds between mating partners[9,14–16]. Comparative studies of closely related species that display distinct patterns of social behaviors, including social monogamy, reveal correlated species-specific differences in the nonapeptide hormones oxytocin (Oxt) and arginine vasopressin (Avp), or their homologs, suggesting that these hormones serve as critical modulators of affiliative behaviors and pair bonding[9–11,16–20]. Despite the central role of social attachment in human behavior and a rich history of investigation into the cognitive processes underlying social cognition and affiliative behaviors, it has been difficult to probe the neural mechanisms underlying these fascinating behaviors at the cellular, molecular, and genetic level, as most species that serve as model organisms for such studies in the laboratory do not display long-term social attachment as adults [6,21–27].

Prairie voles (*Microtus ochrogaster*) display long-term social attachment such that mating partners show an enduring pair bond and social monogamy[13,28–31]. Like many complex innate behaviors, pair bonding consists of distinct modules: the development of increased prosocial behaviors with partners over strangers (partner preference), and increased

agonistic behaviors towards novel opposite sex potential mates (stranger rejection)[13,30,32–37]. As in humans and other species that show affiliative social behaviors, disruption of pair bonds results in increased anxiety-like behaviors and markers of stress, supporting integrated neural and physiologic mechanisms that facilitate the preservation of such attachments[38–40]. Pioneering work in prairie voles identified Oxt and Avp as critical mediators of pair bonding[41,42]. Interspecific variations in the patterns of expression of the oxytocin receptor (Oxtr) and the vasopressin 1a receptor (V1ar) correlate with the potential for pair bonding within closely related vole species[43–49].

Across phyla, manipulations of oxytocin or its species-specific homolog alters social behaviors. In prairie voles, pharmacologic inhibition of Oxt and Avp signaling via their respective cognate receptors disrupts pair bonding, while exogenous administration of these hormones promotes pair bonding without mating[28,50,51]. Transient blockade of Oxtr only during the first few hours of cohabitation delays the formation of a partner preference[28,29] and artificial overexpression of Oxtr accelerates the formation of a pair bond[52]. Exogenous oxytocin administration leads to to increased prosocial behaviors towards conspecifics as well as humans in domestic dogs, initiation of huddling towards a potential partner in marmosets (*Callithrix penicillata*), and food sharing with conspecifics in pinyon jays (*Gymnorhinus cyanocephalus*, a highly social corvid species)[53–56]. Conversely, OT receptor antagonists administered during early pair-bond formation to monogamous cichlid fish (*Amatitlania nigrofasciata*), socially monogamous zebra finch (*Taeniopygia guttata*) and marmosets (*Callithrix penicillata*) lead to reduced affiliative behaviors towards potential mates[55,57,58]. Taken together, these studies underscore the

117 broad conservation of this neuropeptide in the modulation of social behaviors, as well an
118 early temporal window during which oxytocin-dependent behaviors mediate partner
119 preference.
120
121 Given the central role of Oxt signaling in affiliative behaviors, we tested the genetic
122 requirement for signaling via Oxtr for pair bonding and social behaviors in prairie voles.
123 We generated prairie voles lacking Oxtr and unexpectedly observed that these animals
124 continue to display a strong preference for partners following mating and cohabitation[59].
125 To gain deeper insight into the modulation of attachment and social behaviors by Oxtr
126 function, we developed a series of behavioral assays to probe distinct aspects of pair
127 bonding and associated social behaviors. To interrogate the molecular mechanisms
128 mediating social attachment, we profiled patterns of gene expression in the nucleus
129 accumbens (NAc), a key site of species differences associated with social monogamy
130 that is dramatically enriched for Oxt binding in prairie voles[45,60,61]. We find that Oxtr
131 controls the timing of pair bonding in prairie voles and promiscuity independent of partner
132 preference formation. Oxtr sex-specifically influences the behavior of potential mates,
133 increasing agonistic displays in naive wildtype (WT) females, evidenced by decreased
134 aggression and increased prosocial interactions shown by potential female WT mates in
135 the presence of a male lacking Oxtr. Oxtr function regulates patterns of gene expression
136 in the NAc, as well as other regions of the vole brain implicated in social and attachment
137 behaviors, in distinct ways in each sex. Furthermore, we see changes in expression of
138 genes regulating neurodevelopmental processes and disease, supporting a role for Oxtr
139 function early in life[62–64]. Finally, consistent with potential trophic effects of Oxtr function

140 during development, we find that loss of Oxtr alters patterns of Oxt and Avp expression
141 in the paraventricular nucleus, a principal source of these neuropeptides[63,65]. Our studies
142 reveal genetically separable components of pair bonding and suggest that Oxtr signaling
143 sex-specifically participates in the development of the circuits underlying attachment
144 behaviors.

145 **Results**

146 **Oxtr function facilitates the formation of partner preference**

147 We previously found that partner preference formation, following 1 week of cohabitation,
148 can occur in the absence of Oxtr function[59]. However, acute modulation of Oxtr signaling
149 can alter patterns of social behaviors between individuals[29,50,66]. These observations
150 suggest that changes in Oxtr function may influence early social interactions that
151 contribute to the trajectory of pair bond formation and/or specific aspects of attachment
152 behaviors following the formation of partner preference. We first wished to determine
153 whether Oxtr function facilitated pair bond formation by examining the display of partner
154 preference following shorter periods of cohabitation. Consistent with previous studies
155 showing that the cohabitation time required for the display of partner preference differs
156 between males and females, we find that WT females demonstrate partner preference
157 after only 6 hours of cohousing with a WT male partner, while WT males require 5 days
158 following introduction to a potential WT mate (Fig. S1A-C)[67]. We therefore cohoused WT
159 or $Oxtr^{1-/-}$ females with WT males for 6 hours, and WT or $Oxtr^{1-/-}$ males with WT females
160 for 5 days following introduction (short cohabitation), or in these combinations for 1 or 7
161 days (long cohabitation) for females or males, respectively (Fig. 1A, Fig. S1A).
162

163 Both males and females lacking Oxtr show an absence of partner preference following
164 short cohabitation with WT partners (Fig. 1B). Oxtr$^{1-/-}$ females, but not males, showed a
165 decrease in the fraction of huddling time with their partner and an increase in the fraction
166 of huddling time with a stranger compared to WT controls (Fig. 1C-D). Oxtr$^{1-/-}$ males
167 present an absence of partner preference (Fig. 1B), resulting from a trend towards
168 decreased time with their cohoused partner and increased time with strangers (Fig. 1C-
169 D). Consistent with our previous studies, we find no difference between WT and Oxtr$^{1-/-}$
170 females when the pairs are cohoused for the longer duration (Fig. S1B-F).
171
172 To better understand the social interaction dynamics underlying differences in huddling
173 behavior between WT animals and their siblings lacking Oxtr after short-term
174 cohabitation, we quantified the cumulative time subjects spent huddling with either their
175 cohoused partners or strangers across the assay.Oxtr$^{1-/-}$ females show a significant
176 decrease in the amount of time spent huddling with partners in the last 30 mins of the
177 assay (150-180mins) (Fig. 1E). We also observe a significant increase in huddling time
178 of Oxtr$^{1-/-}$ males with strangers during the middle periods (75 – 130mins) (Fig. 1F),
179 suggesting that they engage in more early prosocial behavior with strangers than WT
180 males. Consistent with our previous work, we find no difference between cumulative
181 huddling times with either partner or stranger between WTs and Oxtr$^{1-/-}$ animals of both
182 sexes after long cohabitation periods (Fig. 1G-H)[45]. These observations demonstrate that
183 Oxtr function changes the temporal dynamics of social interactions with both familiar and
184 unfamiliar animal in a sex-specific manner. Taken together, our findings suggest that Oxtr

185 function acts early in the process of pair bonding to facilitate the formation of the partner
186 preference.
187

188 **Oxtr suppresses promiscuous behaviors in a state dependent manner in females**

189 Oxtr influences the dynamics of interactions with partners and strangers differently
190 between the sexes. We therefore wished to examine the detailed patterns of these
191 interactions separately in females and males (Fig. 2A). We examined the distribution of
192 huddles by WT vs Oxtr$^{1-/-}$ females following short cohabitation as a measure of prosocial
193 behavior displayed by these animals. We find that the top quartile of huddle durations
194 (long huddles) from each subject animal make up an average of ~90% of the total huddle
195 duration, functionally separating these interactions from incidental side-by-side contact
196 that may not constitute affiliative huddling (Fig. S2A Left). We classified long huddles as
197 partner huddles or stranger huddles and discovered that, consistent with the overall time
198 spent, the median huddle duration carried out by Oxtr$^{1-/-}$ females is significantly shorter
199 with partners and significantly longer with strangers, compared to WT females (Fig. 2B).
200 The longest huddle displayed with partner is significantly longer for WT females compared
201 to Oxtr$^{1-/-}$ females though we find no difference in the length of the overall longest huddle.
202 This is due to some Oxtr$^{1-/-}$ females conducting their longest huddle with the stranger
203 instead (Fig. S2B). Oxtr$^{1-/-}$ females additionally executed a larger number of huddles only
204 with the stranger, but not the partner, compared to WT controls (Fig. 2C). Taken together,
205 these results suggest that Oxtr function in females both facilitates prosocial behavior with
206 partners and suppresses such behavior with strangers during the early stages of pair
207 bond formation.

208

209 We next wished to determine whether the loss of Oxtr function influences patterns of
210 prosocial behaviors after the display of partner preference. We therefore examined
211 patterns of huddling, in particular the duration and frequency of these interactions,
212 following long cohabitation, a time point at which both WT and Oxtr$^{1-/-}$ animals display
213 robust preference for partners over strangers[59] (Fig. S1D). As with short cohabitation, the
214 top quartile of huddles (by duration) for each subject animal following long cohabitation,
215 described an average of 90% of total huddle time (Fig. S2A right). Following long
216 cohabitation, preference and huddling behavior in Oxtr$^{1-/-}$ females is indistinguishable
217 from their WT siblings (Fig. 2D-E). Comparing changes in the frequency of top quartile
218 huddles displayed by Oxtr$^{1-/-}$ females after short vs long cohabitation, we find that both
219 WT and Oxtr$^{1-/-}$ females show decreased huddle frequency with stranger following long
220 cohabitation (Fig. S2C-D). On comparing durations of long huddles, we find that Oxtr$^{1-/-}$
221 females significantly increase their median huddle duration with partner post long
222 cohousing (Fig. 2F-G). Thus, loss of Oxtr function in females reduces the duration of early
223 prosocial interactions (short cohabitation) with partners and strangers while Oxtr-
224 independent mechanisms eventually promote WT patterns of affiliative huddling and
225 partner preference following longer periods of cohabitation.

226

227 Our results suggest that Oxtr function influences specific aspects of early pair bonding
228 and attachment behaviors. We next wished to dissociate the influence of Oxtr on the
229 formation and display of partner preference from the display of agonistic rejection
230 behaviors towards novel strangers following cohabitation. We therefore developed a

231 battery of assays to examine initial social interactions between mating partners at early
232 and later stages of pair bonding, as well as stranger rejection following cohabitation
233 (Fig.2A). We examined the behavior of subject females from each genotype with WT
234 males when naive animals were first introduced to each other (Introduction), mating
235 behaviors following estrus induction (Timed Mating), prosocial interactions following
236 reunification with their bonded mate (Partner Reunification), and agonistic rejection of
237 novel, opposite sex strangers (Stranger Rejection) (Fig. 2A see Methods). We find no
238 differences in social behaviors during Introduction, Timed Mating and Partner
239 Reunification (Fig. 2H-J). In contrast, during Stranger Rejection, Oxtr$^{1-/-}$ females show
240 more social behaviors towards novel naive males than WT females do in the absence of
241 their partner (Fig. 2K). Taken together, these studies demonstrate that Oxtr function
242 regulates specific components of pair bonding in females in a state-dependent manner,
243 suppressing promiscuous social interactions with stranger males after cohabitation
244 sufficient for the display of partner preference.
245

246 **Oxtr function influences different prosocial behaviors across the stages of pair**
247 **bonding in males**

248 Given the Oxtr-dependent difference in huddling behavior between males and females
249 after short cohabitation (Fig. 1C-D), we wished to assess sex differences in the patterns
250 of behaviors displayed by Oxtr$^{1-/-}$ animals and to further investigate Oxtr function in males
251 (Fig. 3A). Examining long huddles (as above, Fig. 2), we find that such huddles by Oxtr^{1-}
252 $^{/-}$ males with their partners following short cohabitation are significantly shorter when
253 compared to WT siblings, contributing to diminished partner preference early in pair

254 bonding (Fig. 3B Left). Interestingly, while Oxtr$^{1-/-}$ males show no difference in the total
255 amount of time spent huddling with strangers when compared to WT siblings (Fig. 1D),
256 they display shorter and more frequent huddles towards them at this time (Fig. 3B, 3C
257 Right). In males, Oxtr thus influences the pattern as well as amount of early affiliative
258 behavior to distinct behavioral stimuli in different ways.
259
260 Oxtr$^{1-/-}$ males show no difference in time spent with either partners or strangers after long
261 cohabitation (Fig. S1E-F). However, these males show a persistent reduction in the
262 duration of their long huddles with strangers at this time point (Fig. 3D). Following long
263 cohabitation, WT and Oxtr$^{1-/-}$ males show no difference in the duration of long huddles
264 with partners and a reduction in the duration of long huddles with strangers (Fig. S3A-B).
265 We find no difference in the frequency of long huddles between Oxtr$^{1-/-}$ and WT males
266 after long cohabitation (Fig. 3E). Consistently, comparing Oxtr$^{1-/-}$ males' behavior following
267 short vs long cohabitation reveals that the frequency with which Oxtr$^{1-/-}$ males huddle with
268 strangers decreases following long cohabitation (Fig. 3F-G). Thus, specifically in males,
269 loss of Oxtr function does not change the overall time spent huddling with strangers after
270 short or long cohabitation but does cause a continuing disruption in the patterns of
271 affiliative behavior that comprises huddling with strangers.
272
273 Our observations suggest that the loss of Oxtr disrupts certain characteristics of prosocial
274 behaviors in males regardless of the time spent bonding with their partner. We next
275 wished to dissect whether such loss of function resulted in atypical affiliative or agonistic
276 behaviors across stages of bonding. We examined the behavior of Oxtr$^{1-/-}$ males and their

277 WT siblings in the same series of paradigms described previously to characterize the
278 formation and maintenance of their pair bonds (Fig. 3A). Oxtr$^{1-/-}$ males spend similar
279 amounts of time as WT males engaging in prosocial behaviors with partners regardless
280 of bonding state (Fig. 3H-J, S3E). Similar to our observations in Oxtr$^{1-/-}$ females, Oxtr$^{1-/-}$
281 males spend more time engaging in prosocial behaviors with strangers in the absence of
282 their partners (Fig. 3K).
283
284 In contrast to time spent conducting mating behaviors with WT female partners (Fig. S3E),
285 Oxtr$^{1-/-}$ males demonstrate increased frequency of mating attempts when these females
286 are in estrus (Fig. 3I). Examining all instances of mounting, we find that Oxtr$^{1-/-}$ males
287 carry out shorter mounting bouts more frequently than WT males (Fig. S3F). To determine
288 whether the shorter bouts of mounting in Oxtr$^{1-/-}$ males influence the receptivity of their
289 partners, we compared the mount-to-intromission ratio for each animal[68] and find that
290 females are equally receptive to Oxtr$^{1-/-}$ males as their WT siblings (Fig. S3G). Thus,
291 consistent with our previous observations, Oxtr influences patterns, but not the amount
292 or success, of male mating behaviors, suggesting that such changes in males' behaviors
293 are equally able to elicit receptivity in females.
294
295 Oxtr function influences distinct components of males' attachment-related social
296 behaviors towards unfamiliar females at different stages of pair-bonding, lengthening
297 mating bout durations when naïve and suppressing promiscuous prosocial behaviors
298 upon bonding. Taken together our results suggest that Oxtr influences patterns of social
299 behaviors with future partners during the early phases of pair-bonding differently in

300 females and males, but upon bond formation, functions in both sexes to suppress
301 promiscuous affiliative behaviors towards strangers (Fig. S3H).
302
303 **Oxtr sex-specifically influences social interactions between potential mates**
304 Oxtr function influences patterns of social interactions between mates early during the
305 formation of a pair-bond (Short Cohabitation in both sexes, Introduction and Timed Mating
306 in males). We therefore investigated the effect of Oxtr loss on the choice made by a
307 potential mate. We developed a variation of the PPT three-chamber assay to present a
308 naive WT "chooser" with a choice between a naive opposite sex WT or naive opposite
309 sex $Oxtr^{1-/-}$ animal (Fig. 4A, Fig. S4A, see Methods). Using the "naïve-choice" paradigm
310 we find that, over the course of 6 hours, WT choosers spend significantly more time with
311 one of the two stimulus animals (winner) (Fig. 4B) and that WT and $Oxtr^{1-/-}$ animals are
312 chosen as the winner with equal frequency(Fig. 4C).
313
314 To examine whether Oxtr influences the dynamics of the choice made by a potential WT
315 mate, we compared the time spent with the winner from a lane where the chooser had a
316 choice between a naïve WT or $Oxtr^{1-/-}$ animal (WTOxtr lanes) versus that of a chooser
317 choosing between 2 naive WT animals (WTWT lanes) of the opposite sex (Fig. 4D). While
318 naïve WT choosers show no difference in overall social choice between naive WT and
319 $Oxtr^{1-/-}$ opposite sex animals (Fig. 4C), WT female choosers show distinct behavioral
320 dynamics in the presence of an $Oxtr^{1-/-}$ male (WTOxtr lane). In the presence of an Oxtr
321 mutant (WTOxtr lane), WT females spend significantly more time in contact with the
322 winner, regardless of genotype, when compared to contact with the winner between two

323 WT males (WTWT lane) (Fig. 4E). In contrast, we observe no difference in contact time
324 with a winner when a naive WT male is choosing in WTOxtr versus WTWT lane (Fig. 4E).
325
326 We therefore manually examined the specific behaviors shown by female WT choosers
327 during their interactions with both the winner and loser in WTWT and WTOxtr lanes.
328 Preference indices using these metrics were highly concordant with automated scoring
329 (Fig. S4A). The time spent by the female chooser displaying prosocial behaviors towards
330 the winner and the time spent huddling with the winner in WTOxtr lanes was significantly
331 greater than WTWT lanes (Fig. S4B) (Fig. 4E). The divergence between the amount of
332 cumulative time spent huddling with the winner from WTOxtr versus WTWT lanes occurs
333 after 5 hours have elapsed (313-360 mins, Fig. 4F), suggesting that complex interactions
334 in the presence of a male lacking Oxtr influence how females "choose" a male partner
335 regardless of whether they end up choosing a WT or $Oxtr^{1-/-}$ winner.
336
337 We evaluated the duration of the longest huddles conducted by all WT female choosers,
338 and find that the longest huddle is always conducted with the winner. The longest huddles
339 conducted in the WTOxtr lanes, regardless of the genotype of the male winner, are greater
340 than those from WTWT lanes (Fig. 4G). There is no difference in the latency to start the
341 longest huddle between WTOxtr and WTWT lanes (Fig. S4C). Thus, the presence of the
342 $Oxtr^{1-/-}$ male in the lane leads a WT chooser female to execute the longest huddle for a
343 greater amount of time compared to the longest huddle by the WT female chooser from
344 a WTWT lane (Fig. 4G). These observations suggests either that naïve $Oxtr^{1-/-}$ males
345 elicit longer longest-huddle bouts from WT females, even when this huddle occurs with a

346 WT male winner, or that the behavior of naïve WT males reduces the duration of WT
347 females' longest huddle - a reduction that is absent in the presence of a male lacking Oxtr.
348
349 To determine if specific patterns of behavior preceded the longest huddle with a winner,
350 we aligned the onset of the longest huddle for all the WTOxtr and WTWT lanes and
351 evaluated the behaviors performed 15 mins prior to its initiation. We find that the duration
352 of sniffs (anogenital investigation, see methods) by WT female choosers in WTWT lanes
353 is greater than those by choosers in WTOxtr lanes (Fig. 4H). We did not find any
354 difference in the duration of sniffs specifically with the winner or the loser when comparing
355 WTWT and WTOxtr lanes, or in the total time spent sniffing over the course of the assay
356 (Fig S4D, E). Thus, the interactions with both winner and loser contribute to the increase
357 in duration spent sniffing 15 minutes prior to the longest huddle in WTWT lanes. These
358 observations may suggest that a female chooser from the WTWT lane continues to seek
359 chemosensory input before the longest huddle and these huddles are shorter due to
360 ambivalence in a choice between two WT males. In contrast, a WT female chooser in a
361 WTOxtr lane may encounter larger differences between a WT versus $Oxtr^{1-/-}$ male, leading
362 to a display of more prosocial behavior towards the chosen male independent of the
363 winner's Oxtr function.
364
365 We next examined antagonistic behaviors displayed during the naive choice assay as
366 such behaviors may reduce prosocial behaviors displayed by chooser females. We found
367 no difference in the overall counts of aggressive behaviors between WTWT and WTOxtr
368 lanes (Fig. S4F). However, WT female choosers attack the loser male in the WTWT lanes

369 more compared to WTOxtr lanes (Fig. 4I, Fig. S4G). Thus, in WTWT lanes, winner
370 selection may be influenced by the level of aggression elicited by naïve WT males, a
371 factor that is lower in WTOxtr lanes. We find a correlation between the amount of time
372 spent socializing (with both winner and loser) and the count of all the aggression during
373 the assay (Fig. 4J). Female choosers from WTOxtr lanes tend to spend more time
374 engaged in prosocial behaviors with the winner (Fig. 4E-F, S4B) and display inceased
375 prosocial and reduced aggressive behaviors. Female choosers choosing between two
376 WT males, however, display either high prosocial and low aggressive behaviors or low
377 prosocial behavior and high aggression. These observations suggest that the presence
378 of a second male may influence the behavioral state of a WT female. The presence of
379 only WT males may induce aggression by females against eventual losers, while such
380 displays are absent in the presence of a male lacking Oxtr regardless of a female's choice.
381
382 Given the differences in the influence of the presence $Oxtr^{1-/-}$ males on displays of
383 aggression by WT females when choosing between males, we examined antagonistic
384 behaviors exhibited during interactions between naive (Introduction) or bonded (Stranger
385 Rejection) females with WT or $Oxtr^{1-/-}$ males in the absence of a third animal. Strikingly,
386 we find that counts of aggressive behaviors were elevated only when naive WT females
387 encountered WT males compared to $Oxtr^{1-/-}$ males, while this difference is lost following
388 pair bonding (Fig. 4K). In contrast, we find no differences in aggressive behaviors when
389 comparing naïve or bonded WT and $Oxtr^{1-/-}$ females (Fig. S4H). Taken together, these
390 data suggest sex- and state-specific roles for Oxtr function. Specifically, in naive males,
391 Oxtr function induces displays of aggression by naive females, and the presence of a

392 male lacking Oxtr diminishes a naïve WT female's propensity to display agonistic
393 behaviors even in the presence of a WT male. Following bonding, however, the absence
394 of Oxtr function in males does not appear to influence the behavior of WT females despite
395 the promiscuous prosocial displays such mutant males.
396
397 Finally, to determine if naive prairie voles lacking Oxtr display generalized changes to
398 their behaviors independent of attachment-associated social behavior, we examined
399 general pro-social, anxiety-related, and locomotor behaviors. With the exception of an
400 increase in locomotion displayed by $Oxtr^{1-/-}$ females when compared to WT females in
401 an open field paradigm, we found no differences between $Oxtr^{1-/-}$ and WT voles of either
402 sex (Fig. S4I).
403
404 We have examined social interactions during the initial contact between mates, the
405 early stages of pair bonding, and during social attachment behaviors following partner
406 preference formation. Consistent with our findings and previous work, Oxtr function is
407 not required for the eventual display of partner preference. Here, we demonstrate that
408 Oxtr function sex-specifically facilitates early social interactions that contribute to the
409 formation of partner preference, and controls promiscuity.
410
411 **Oxtr controls the molecular signature of pair bonding in the nucleus accumbens**
412 While partner preference formation can occur in the absence of Oxtr function, we find that
413 it suppresses prosocial behaviors towards novel strangers following pair bonding. These
414 results suggest that distinct components of pair bonding are differentially influenced by

415 Oxtr function or compensated upon its loss. We next characterized the molecular
416 signature associated with pair bonding to determine whether changes in gene expression
417 following pair bond formation are controlled by Oxtr. Comparative studies demonstrate
418 that Oxt binding in multiple brain regions differs significantly between promiscuous and
419 monogamous rodent species. Oxt binding is particularly enriched in the NAc in prairie
420 voles, while vasopressin binding is largely absent in this area[45,47]. Thus, analyzing gene
421 expression in the NAc allows us to identify bonding-related expression that is primarily
422 due to Oxtr function and largely independent of the direct consequences of AVP signaling.
423 Additionally, given the well-established role of the NAc in the association of reward or
424 aversion with specific sensory and environmental cues[69–71] this region is well poised to
425 play a role in the development of partner preference, even without Oxtr signaling, as well
426 as stranger rejection, which appears to be dependent upon Oxtr function.
427
428 We performed bulk RNA-sequencing on NAc tissue from WT and $Oxtr^{1-/-}$ animals of both
429 sexes that were either: group housed with same-sex peers and sexually naïve (pre-
430 pairing); or paired with WT opposite-sex partners for six days, using our timed mating
431 paradigm (post-pairing) (Fig. 5A). PCA showed robust separation of WT and $Oxtr^{1-/-}$
432 samples (Fig. S5A). Differential expression (DE) analysis of pairing condition, regardless
433 of genotype or sex, identified 13 genes that show significant changes in expression post-
434 pairing (Fig. S5B), all of which showed decreased expression (Fig. 5B). These genes
435 include *Agt, Sgk1, Ptgds, Fosb, Pdk4*, and *Acsm5* (Fig. 5C) and, while these genes have
436 not previously been linked to shared gene regulatory or functional pathways, the predicted
437 protein-protein interaction network for the 13 DE genes shows more connections than

438 would be expected by chance (p=2.47 e^{-05}) (Fig. S5C). Intriguingly, even in the limited set
439 of genes with altered expression in the context of pair bonding, changes are driven
440 primarily by expression in WT females (Fig. 5C, S5D). Subgroup analyses by genetic
441 background and sex identified additional genes including *Adora2a, Fkbp5*, and *Spred3* in
442 WT females and collagen-related genes, including *Col4a1* and *Col4a2*, in $Oxtr^{1-/-}$ females
443 (Fig. 5D, S5D). Only one gene, *Sema3b,* is significantly different in $Oxtr^{1-/-}$ males following
444 pairing (Fig. 5D).
445
446 To further examine changes in patterns of gene expression in the NAc associated with
447 pair bonding, we performed weighted gene coexpression network analysis (WGCNA)[72]
448 and calculated three sets of modules (M) from different sample subsets ($modules^{WT}$,
449 $modules^{Mut}$, and $modules^{All}$) (Fig. S5F, S6D). Using the $modules^{WT}$ subset, we identified
450 15 coexpression modules (Fig. S5F, Table 2) representing genes that share highly similar
451 expression patterns within the NAc. We identified one module ($Mpink^{WT}$) that significantly
452 and specifically correlated with pre-pairing status in WT animals (Pearson R correlation
453 of 0.7, Bonferroni adjusted p-value (p_{adj})=0.018) (Fig. 5E, S5E-F). Genes with high
454 module membership for the $Mpink^{WT}$ are also those with high gene significance for pairing
455 condition supporting the module's association with behavior condition (Fig. 5SG). Further,
456 genes significantly differentially expressed with bonding are significantly enriched in
457 $Mpink^{WT}$ (Bonferroni p_{adj}=7.44 e^{-08}) and serve as hub genes within this module (Fig. S5E,
458 G). These results suggest that the $Mpink^{WT}$ module might be driving, or under the
459 influence of pathways driving, the pre-pairing to post-pairing state change.
460

461 We asked whether any of the modules^{WT} identified were regulated by Oxtr and thus lost
462 in Oxtr null animals. To address this, we assessed how well modules^{WT} are preserved in
463 mutant samples. We calculated a $Z_{summary}$ measure that combines module density and
464 intramodular connectivity metrics into a composite statistic. We find that of the modules^{WT},
465 Mpink^{WT} had the lowest $Z_{summary}$ ($Z_{summary}$ = 2) in Oxtr$^{1-/-}$ samples (Fig. 5F), indicating that
466 dynamics of gene expression that correlate with bonding states are lost in the absence of
467 Oxtr. Finally, the module eigengene (ME) for Mpink^{WT} when calculated for all 30 samples
468 and compared between pre- and post-pairing, was significant only for WT females
469 (Wilcoxon rank sum, Benjamini-Hochberg p_{adj}=0.03) and not for WT males or Oxtr$^{1-/-}$
470 animals of either sex (Fig. 5G). These observations suggest there is sex-specific,
471 coordinated regulation of gene expression in the NAc following pairing of mates that may
472 be associated with pair bond associated behaviors.
473

474 **Loss of Oxtr sex-specifically disrupts patterns of gene expression associated**
475 **with neurodevelopmental disorders**

476 We next wished to determine how Oxtr signaling contributes to changes in gene
477 expression in the NAc associated with the naive state or the process of pair bonding (Fig.
478 6A) by comparing the transcriptional profile of WT and Oxtr$^{1-/-}$ animals of each sex. Given
479 that our lines are maintained on an outbred background, in order to minimize sample
480 variability, tissue from three animals was pooled for each sample. We observed significant
481 genotype specific differences in gene expression in animals from both sexes, with 466
482 genes showing differences between WT and Oxtr$^{1-/-}$ females, 270 between WT and Oxtr^{1-}
483 $^{/-}$ males, and 1,014 genes when samples from both sexes were combined (using a

484 p_{adj}<0.05 and absolute (log_2(FC)) > 0.25 as criteria). Of the combined DE gene set, 370
485 genes are upregulated and 644 are downregulated (Fig. 6B, S6A-B). Genes with the
486 greatest fold change across both sexes include *Slc2a3, Kcna1, Rgs8, Cnksr2, Acvr*, and
487 *Cnot6* (Fig. 6B). Genes specifically downregulated in $Oxtr^{1-/-}$ females with log_2(FC) less
488 than 1 include *Abcb11* (a gene recently associated with treatment resistant
489 schizophrenia[73]), *Ngfr, Pon3,* and *Shh*. While there was no significant difference in Oxtr
490 transcript levels by genotype (p_{adj} = 0.753)—consistent with minimal nonsense-mediated
491 decay despite a premature stop codon—we have previously shown that no functional
492 protein is produced in $Oxtr^{1-/-}$ animals via autoradiography[59]. V1aR showed a modest
493 decrease in expression in $Oxtr^{1-/-}$ animals (p_{adj}=0.03) (Fig. S6C), though this is likely
494 influenced by variability in WT samples. WGCNA of all samples identified two modules
495 ($Mbrown^{All}$ and $Mturquoise^{All}$) that were significantly positively correlated with the WT
496 genotype compared to mutant (Pearson R = 0.55, p_{adj} = 0.011 for brown and Pearson R
497 = 0.8, p_{adj} = 6.6e-7 for turquoise) (Fig. S6D). None of the identified modules showed
498 correlation with pairing condition (Fig. S6D). Our results thus reveal a dramatic change in
499 patterns of gene expression in the NAc with global loss of Oxtr signaling, independent of
500 bonding state.
501
502 Examination of the sets of genes whose expression is altered by the loss of Oxtr,
503 regardless of bonding state or sex, revealed several distinct cellular processes regulated
504 by Oxtr signaling. These processes comprise larger domains of cell function including
505 extracellular channel binding activity, axoneme assembly complex, axon glial
506 ensheathment development, and metal cation transport (Fig. 6C), as well as pathways

507 for G protein signaling and dopaminergic neurogenesis (Fig. S6E). When analyzed by
508 sex, more of the identified processes were enriched in female Oxtr gene sets than in male
509 ones (female: 19/62, male: 6/62). To further link differentially expressed genes to
510 behavioral traits, we asked whether genes altered by loss of Oxtr are selectively enriched
511 for high-confidence associations with autism spectrum disorders (ASD) and other
512 neurodevelopmental diseases (NDD) affecting social attachment in humans as compared
513 to epilepsy, a disorder that does not disrupt social attachment[74–77]. Consistently, we find
514 that the genes upregulated with loss of Oxtr ($p_{adj}<0.01$, $\log_2(FC)>0$) are specifically
515 enriched for ASD- and NDD-associations but not epilepsy associations (Fig. 6D "Joint").
516 This enrichment is again primarily driven by genes upregulated in females and not males
517 (Fig. 6D). Thus, similar to the factors that influence gene expression changes associated
518 with pair bonding, many of the changes we identify in the NAc resulting from loss of Oxtr
519 are primarily driven by female-specific effects that may play a conserved role in mediating
520 social attachment in humans.
521

522 **Oxtr regulates coordinated gene expression across multiple neural populations**
523 **implicated in social attachment behaviors**

524 Given the expression of Oxtr in regions of the brain known to mediate social behavior in
525 voles and other species[78,79], we wished to determine if genes whose expression is altered
526 in the NAc by the loss of Oxtr were expressed not only in specific populations of cells
527 within this region, but in other regions of the prairie vole brain implicated in social and
528 attachment behaviors. We therefore examined the expression of 15 genes that showed
529 significant changes in expression in WT females when compared to those lacking Oxtr

using *in situ* hybridization (ISH) to both validate our RNA-seq findings as well as examine the expression patterns of these genes. Several of these genes, such as phosphodiesterase 10A (*Pde10A)* and diacylglycerol kinase beta (*Dgkb)*, show robust expression throughout the striatum (data not shown), while genes such as the calcitonin receptor (*Calcr*) and delta like non-canonical notch ligand 1 (*Dlk-1*) are expressed in restricted populations of cells in the NAc (Fig. 6F-H, top panels). The expression of these genes is significantly reduced in $Oxtr^{1-/-}$ females (Fig. 6E-H), supporting the specificity and resolution of our RNA-seq findings.

In parallel to our examination of gene expression in the NAc, our ISH revealed that loss of Oxtr in females altered the expression of the genes we examined in other regions of the prairie vole brain. We examined the expression of these genes in the lateral septum (LS), a region that has been implicated in agonistic and attachment behaviors in prairie voles and other rodents and shows species dimorphic patterns of Oxt and Avp binding. We observe that both *Calcr* and *Dlk-1* are decreased in the absence of Oxtr (Fig. 6G, H middle panel) in the LS. We also find that expression of *Calcr* and *Dlk-1* is decreased in the paraventricular nucleus of the hypothalamus (PVN), a principal source of Oxt and Avp in the rodent brain which sends projections to the NAc (Fig. 6G-H bottom panels)[80–82]. These findings suggest that Oxtr function regulates patterns of gene expression in multiple regions of the brain implicated in social and attachment behaviors in a coordinated and region-specific manner.

552 **Loss of Oxtr results in the decrease in density of Oxt and Avp expressing**
553 **neurons in the PVN**

554 We find here that loss of Oxtr results in coordinated changes in gene expression in
555 multiple neural populations, including the PVN. We therefore wished to determine if the
556 signatures of gene expression regulated by Oxtr in the NAc in prairie voles (ONP set),
557 regardless of sex and bonding state, were enriched for patterns of gene expression
558 associated with distinct neural populations in other regions of the brain, particularly those
559 implicated in social and attachment behaviors. We compared the ONP gene set to the
560 molecular signatures of 33 hypothalamic subtypes previously identified by single-cell RNA
561 sequencing in mice[83]. Of the 33 clusters examined, the four with highest overlap with the
562 ONP gene set represent subsets of PVN neurons, in particular those that express Oxt
563 and AVP (Fig. 7A, clusters 43 and 26), as well as PVN neurons that express *Dlk1* and
564 *Calcr* (cluster 29), both of which show reduced expression in the NAc and PVN in females
565 lacking Oxtr (Fig. 6G-H bottom panel).
566

567 We next sought to determine if the overlap between Oxtr regulated genes and gene
568 expression patterns of neural populations in the PVN correlated with changes in the
569 expression of neuropeptides within PVN itself. We examined patterns of Oxt and Avp
570 expression using immunohistochemistry in naive adults and compared patterns of
571 expression between WT animals of both sexes and those lacking Oxtr (Fig. 7B, Fig.
572 S7A-B). We find that the density of both Oxt and Avp producing neurons is lower in
573 $Oxtr^{1-/-}$ animals (Fig. 7C-E). To determine if the loss of Oxt or Avp expression was
574 restricted to specific populations of PVN neurons, we examined the expression of these

575 peptides across the anterior-posterior axis of the PVN in both WT and Oxtr$^{1-/-}$ males and
576 females. We find that animals of both sexes show a preferential loss of Oxt and Avp
577 expressing neurons in the anterior PVN (Fig. 7F-G). Finally, we examined patterns of
578 Oxt and Avp over the course of development to determine when loss of Oxtr function
579 influences the development of their expression. We find that the density of Oxt neurons
580 at P0 (Fig. S7C-F) and both Oxt and Avp neurons at P21 is lower in Oxtr$^{1-/-}$ females
581 compared to age matched WT females (Fig. S7G-J). In contrast, we find that Oxt and
582 Avp neuron density loss occurs only in adult Oxtr$^{1-/-}$ males (Fig. 7D-G, Fig. S7B). These
583 observations suggest the coordinated, region-, and sex-specific influence of Oxtr
584 function on the development of neurons expressing Oxt (and Avp) within the PVN,
585 consistent with a trophic role for this pathway identified in mice[63,65,84,85].
586

587 **Discussion**

588 Robust reproductive behaviors are essential for survival. Accordingly, species have
589 evolved diverse strategies, including social monogamy, which mediate locating,
590 identifying, and attracting mates, facilitate reproduction, and promote the survival of
591 progeny[16,86]. Signaling via Oxtr influences a wide range of physiology and behavior
592 associated with social interactions and attachment between conspecifics, including pair
593 bonding between prairie vole mates[41,87]. Acute blockade of Oxtr signaling via central or
594 nucleus accumbens infusions of Oxtr antagonists prevents the formation of partner
595 preference[28,50,51,60,88]. In contrast, constitutive loss of Oxtr in prairie voles disrupts specific
596 components of pair bonding, while the capacity for partner preference ultimately remains
597 intact[59]. Similarly, Oxtr null mice show select behavioral deficits, including impaired

598 sociability, reduced preference for social novelty, and increased aggression towards a
599 novel intruder[89,90].Thus, like other circuit and neuromodulatory pathways across diverse
600 species, Oxtr likely functions in parallel to multiple genetically specified pathways to
601 influence specific behavioral modules that comprise complex behavioral states, including
602 social attachment.[33,35,91–97]. These actions are likely dependent on the developmental
603 context and engagement of potentially compensatory parallel pathways, leading to
604 divergent phenotypes depending on the timing and nature of Oxtr disruption.
605
606 Here we demonstrate that loss of Oxtr in prairie voles influences the dynamics of social
607 interactions between sexually naïve animals and WT potential mates in distinct social
608 contexts in sex-specific ways. The presence of a naive $Oxtr^{1-/-}$ male changes levels and
609 patterns of both early prosocial and antagonistic behaviors displayed by naive WT
610 females, supporting the role of Oxtr in controlling individuals' and reciprocal behavior [30].
611 Thus, Oxtr function orchestrates male social behaviors operating early in the sensitive
612 period of pair-bond formation and, through these behaviors or through additional sensory
613 cues yet to be identified (pheromone signatures or vocal communication), shapes
614 bonding.
615
616 Animals lacking Oxtr take longer to display partner preference, and despite strong partner
617 preference following longer cohabitation, demonstrate promiscuous prosocial behaviors
618 towards novel potential mates, including huddling with strangers. These observations are
619 consistent with a state-dependent role of Oxtr function, similar to findings in multiple
620 species, including humans[98–100]. Oxtr function may thus promote prosocial behavior in the

621 naïve state to facilitate attachment with an unfamiliar potential mate, but following pair
622 bond formation, suppresses further prosocial interactions to new individuals, or even
623 promotes further separation from and rejection of unfamiliar individuals or groups. Across
624 species and outside of the context of pair bonding, oxytocin signaling may play a
625 conserved role in mediating other state-specific aversive behavior, for example, defeat-
626 induced social avoidance learning[101].
627
628 Our findings reveal that patterns of social behaviors contributing to 1) pair bond formation,
629 2) partner preference, and 3) rejection of novel mates are genetically separable
630 components of pair bonding representing distinct behavioral modules regulated by
631 mechanisms that require Oxtr function, i.e. reciprocal behaviors and stranger rejection, or
632 those that can be displayed in its absence, i.e. partner preference. Further work will allow
633 us to determine the Oxtr-independent mechanisms that mediate the closure of an early
634 sensitive period and facilitate the display of partner preference[59]. Where Oxtr functions
635 to control the switch from prosocial behavior towards a potential mate in naïve animals to
636 the suppression of such behaviors towards, and active rejection of, opposite-sex
637 conspecific strangers following bonding remains to be determined.
638
639 Examination of the molecular signatures of pair bonding and the role of Oxtr in regulating
640 these changes in gene expression in the NAc reveals modest, Oxtr-dependent changes
641 in the expression of a specific network of genes in WT animals following pair bonding[45,102].
642 Intriguingly, loss of Oxtr preferentially impacts patterns of gene expression in the NAc in
643 females. The NAc demonstrates little endogenous sex steroid hormone receptor

644 expression difference in gene expression in prairie voles and other species[78,103–105]. Sex
645 differences in the effects of Oxtr on gene expression this region may therefore suggest
646 that there are significant sex-differences in the inputs into this region that act through Oxtr
647 during development[106–111]. The larger impact of loss of Oxtr in females is consistent with
648 its more general conservation in mammals to regulate aspects of female physiology such
649 as lactation and prosocial behaviors or sensory cues that promote interactions with
650 males[112].
651
652 Oxt and its receptor show species-specific changes in expression through embryonic
653 development and early postnatal life, impacting the development of cortical and
654 subcortical circuits[62,64,113,114]. Consistent with this, genes with altered expression in the
655 absence of Oxtr are enriched for genes associated with neuropsychiatric disorders, in
656 particular neurodevelopmental disorders and ASD. Given the sex-biased enrichment of
657 these genes, such developmental differences in the impacts of Oxtr function may
658 contribute to sex differences in the pathophysiology of these disorders[115–117]. Accordingly,
659 the molecular signatures of attachment in the NAc, both dependent upon and
660 independent of Oxtr function, are subtle relative to these sex-biased differences in the
661 role of Oxtr and possibly reside in other neural populations that function in attachment.
662
663 Validation of changes in gene expression in the NAc resulting from loss of Oxtr suggests
664 coordinated regulation of these genes by Oxtr across multiple brain regions implicated in
665 social and attachment behaviors. Oxtr may be one of multiple factors that organizes
666 specific components of the circuits underlying these displays to control discreet modules

667 of behavior. Consistent with a trophic role for Oxtr function during development, we find
668 that the genes regulated by Oxtr within the NAc are enriched for those that identify cell
669 types in the PVN, a principal source of neuropeptides implicated in pair bonding, which
670 sends oxytocinergic projections to the NAc[79,81,118–120]. Neonatal OT manipulations in mice
671 sex-specifically modulate levels of neuropeptides in PVN neurons, increasing Oxt
672 expression in females and reducing Avp expression in males[64]. We demonstrate that, in
673 prairie voles, loss of Oxtr preferentially impacts Oxt and Avp expression in the anterior
674 PVN, suggesting that specific populations of these cells may be more dependent upon
675 such trophic function for their development, survival, or expression of these hormones.
676 Whole brain analysis will likely reveal if such neurons have distinct projections when
677 compared to those that remain in the absence of Oxtr, contributing to our understanding
678 of how these circuits and pathways regulate distinct aspects of social and attachment
679 behaviors and physiology[4,87,121].
680
681 Taken together, our behavioral and molecular studies reveal previously unappreciated
682 nuances in the control of social behavior and pair bonding by Oxtr function. They uncover
683 intriguing sex differences in the patterns of behavior influenced by loss of Oxtr function.
684 These observations suggest that circuits with sex-specific patterns of development, or
685 even function in ancestral species, may mechanistically converge in the context of Oxtr
686 function to generate displays of reciprocal interactions, pair bonding and attachment
687 behaviors in WT prairie voles that are similar between males and females[122,123].
688 Manipulation of Oxtr expression at specific developmental timepoints and in specific
689 neural populations will help to elucidate how this pathway influences social and

690 attachment behaviors in the context of normal development to regulate distinct
691 components of pair bonding. Understanding the specific neural populations that express
692 Oxtr and other molecular pathways that contribute to pair bonding will allow us to
693 understand the mechanisms controlling the early experience-dependent, sensitive period
694 of bond formation. In parallel, examination of the activity in these populations following
695 manipulations of Oxtr function will allow us to determine the circuit mechanisms by which
696 similar but distinct sensory cues contribute to the identification of partners or novel
697 conspecifics and consequently, the display of dramatically different patterns of social
698 behaviors. The sum of these mechanisms represents the preference for partners over
699 strangers and reflects the formation and maintenance of pair bonds between mates,
700 affiliation between individuals, and the behavioral consequences of identifying others as
701 unfamiliar or outside of these bonds.
702

703 **Acknowledgments**

704 The authors would like to thank members of the Manoli lab for assistance, advice,
705 helpful discussion and comments on the manuscript. J. Tollkuhn and M. Brainard
706 provided valuable insights to the structure, content and design of the manuscript.
707 Additionally, we would like to thank S. Garg for his assistance in data analysis and help
708 designing the analytic pipeline. The authors received funding from National Institutes of
709 Health grant R01MH123513 (D.S.M.), National Science Foundation grant 1556974
710 (D.S.M.), Burroughs Wellcome Fund 1015667 (D.S.M.), Whitehall Foundation grant
711 2018-08-83 (D.S.M.), One Mind Foundation A137726 (D.S.M.), National Institutes of
712 Health grant R25MH060482 (K.M.B.), AP Giannini Foundation Fellowship P0534952

713 (K.M.B.), Larry L. Hillblom Foundation Fellowship 2020-A-023-FEL (K.M.B.), and
714 National Institute of Mental Health grant R01MH123178 (K.S.P.)
715

716 **Author contributions**

717 Conceptualization, R.S., K.M.B., K.L., and D.S.M.; methodology, A.B., A.J.W., D.S.M.,
718 K.L.B., K.M.B., K.S.P., and R.S.; software, K.Q., and S.W.; formal analysis, A.E., R.S.,
719 and K.M.B.; investigation, R.S., K.M.B., A.E., B.W., G.W., S.W., K.Q., R.D.L., K.L., N.H.,
720 B.A.S., M.C.H., M.S., R.K., A.C., D.G., L.C.C., N.L.G.; visualization, R.S., K.M.B., B.W.,
721 and A.E.; funding acquisition, D.S.M., K.S.P., and A.J.W; writing– original draft, R.S., and
722 K.M.B.; writing-review & editing, R.S., K.M.B., D.S.M., N.H., K.S.P., A.E., and A.B.

723 **Declaration of interests**

724 The authors declare no competing interests.
725

726 **Star Methods**

727 **Key resources table**

REAGENT or RESOURCE	SOURCE	IDENTIFIER
Chemicals, peptides, and recombinant proteins		
DAPI	Sigma-Aldrich	Cat #D9542; CAS #28718-90-3

Experimental models: Organisms/strains		
Prairie vole: OxtR$^{1-/-}$	Berendzen et al.	
Oligonucleotides		
ISH probes	This paper	N/A
Oxtr$^{1-/-}$ genotyping oligos	This paper	N/A
Antibodies		
Oxytocin Polyclonal	Invitrogen	Cat#PA5-26701; RRID
Anti-Neurophysin 2/NP-AVP	Millipore	Cat#MABN845; RRID
Cy™3 AffiniPure Donkey Anti-Rabbit IgG	Jackson ImmunoResearch	Cat #711-165-152; RRID
Alexa Flour 488 Donkey Anti Mouse IgG	Thermo Fisher Scientific	Cat #711-165-152; RRID
Software and algorithms		
ImageJ	NIH	; RRID: SCR_003070
R (version 1.1.423)	R Core	https://www.r-project.org/
GraphPad Prism (version 7.03)	GraphPad Software	
Boris	Boris	www.boris.unito.it

MATLAB	MathWorks	https://www.mathworks.com/products.html RRID: SCR_001622

728

729 **Resource availability**

730 **Lead contact**

731 Further information and requests for resources and reagents should be directed to and

732 will be fulfilled by the lead contact, Devanand Manoli (devanand.manoli@ucsf.edu).

733 **Materials availability**

734 All unique reagents generated in this study are available from the lead contact upon

735 request.

736 **Data**

737 Transcriptomics data discussed in this publication are accessible through GEO Series

738 accession number GSE279248.

739 **Code**

740 All code used for RNA-seq data processing and differential expression analyses, as well

741 as post-processed expression data, can be found at

742 https://github.com/aseveritt/OXTR_prairie_voles

743

EXPERIMENTAL MODEL AND SUBJECT DETAILS

Animals

Subjects were laboratory-bred prairie voles (*Microtus ochrogaster*) which originated through systematic outbreeding of a wild stock captured near Champaign, Illinois. CRISPR/Cas9 editing was used to generate 2 independent null alleles, $Oxtr^{1-/-}$ and $Oxtr^{2-/-}$, both of which were validated using autoradiography to show loss of receptor function[59] (data not shown). $Oxtr^{1-/-}$ was backcrossed for >7 generations to mitigate any possible off-target effects and this line was used for all subsequent experiments. Sexually naïve male and female animals were group weaned at 21 ± 1 days and separated to group housing with same-sex siblings and age-matched same-sex non-siblings. Voles were maintained under a 14:10 h light-dark cycle in clear plastic cages (45 × 25 × 15 cm) with bedding, nesting material (nestlet), and a PVC hiding tube. Rooms were maintained at approximately 20°C, and food and water were available *ad libitum*.

Breeding pairs were established between two heterozygotes or a homozygous $Oxtr^{1-/-}$ mutant male and heterozygous female partner from a breeding line maintained in the lab. Voles were randomly assigned into experimental groups when they reached 7-9 weeks of age at the start of testing. This study was carried out in accordance with the recommendations in the Guide for the Care and Use of Laboratory Animals published by the National Research Council. The protocol was approved by the Institutional Animal Care and Use Committee at each respective institution.

766 **Genotyping**

767 The following primers were used to amplify a region where XcmI restriction for $Oxtr^1$ or
768 Bpu10I restriction for $Oxtr^2$ determined the genotype of all animals studied. XcmI cuts
769 the mutant allele in the case of $Oxtr^1$ and Bpu10I restricts the WT sequence for $Oxtr^2$.
770 (Forward: ACTGGAGCTTCGAGTTGGAC, Reverse: ATGCCCACCACTTGCAAGTA)

771 **METHOD DETAILS**

772 **Behavior**

773 ***Triadic naive choice assay***

774 The linear three chamber partner preference apparatus with open top and 10 x 32 inch
775 walls[59] was modified to capture the interactions of the naive, freely moving WT subject
776 and the naive, tethered, opposite sex potential partner (either 2 WTs or a WT and an
777 $Oxtr^{1-/-}$) at either end of the chamber. Behaviors were recorded for 6 hours using a top
778 view camera and the videos generated were analyzed using a contour detection
779 algorithm. Specifically, contours were detected on individual video frames using a
780 threshold-based strategy that took advantage of the contrast between dark-colored vole
781 fur coats and light-colored bedding and chamber apparatus. A standalone vole was
782 detected as a single contour, and two voles in physical contact were likewise detected
783 as a single contour. Consistent vole identities across video frames were determined
784 using the Hungarian algorithm. Since the assay began with one vole in each of the three
785 chambers, and since the subject vole remained freely mobile throughout, it was possible
786 to unambiguously assign each contour to a single vole identity (e.g., subject, right
787 chamber, or left chamber) or to that of a pair of voles (e.g., subject and right chamber
788 voles or subject and left chamber vole), resulting in continuous trajectories for each of

789 the three animals. Time in chamber was determined by the chamber location of the
790 subject vole in each frame, since the chamber location of the right chamber and left
791 chamber animals was fixed throughout the assay by physical tethering and any time the
792 contour of the subject animal merged with that of the tethered animal (right or left), the
793 subject was termed in contact with it. The algorithm also determined the boundaries of
794 the chambers and calculated chamber times. We used the chamber time data from
795 when both ends of the chamber contained tethered WTs (WT-WT condition) to ensure
796 that there was no bias in which side the choosers preferred. This footage was then
797 scored manually to produce greater resolution of behaviors.
798
799 ***Bond formation assays***
800 Initial introduction of $Oxtr^{1-/-}$ and WT animals of either sex with an opposite sex WT animal
801 was filmed for 30 minutes. Observed behaviors included anogenital sniffing, investigation
802 (subject animal's nose contacts any non-genital region), duration of stationary huddling
803 or >50% side-by-side contact between animals, rearing, frequency of aggressive behavior
804 including lunges, receipt of aggression, and tussles, as well as mating behavior including
805 mounting, intromission, and ejaculation. These animals remained in their home cage for
806 18 hours following pairing, after which, they were separated by a clear, plastic barrier. The
807 barrier was left in place for 24 hours and then removed allowing the subject free access
808 to the partner animal thereafter. A 30-minute period directly following barrier removal was
809 also filmed to assess mating behavior, termed the timed mating assay.
810

811 Subjects remained cohoused with the opposite-sex, wildtype partner for durations as
812 indicated in the text. The partner preference test (PPT), as previously published[59], was
813 used to assess pair bond formation. Subject, partner, and an opposite sex stranger are
814 placed in a three-chamber apparatus with open top and 10 x 32-inch walls. The partner
815 and stranger animals are tethered on either end of the three-chamber arena and the
816 subject allowed free access over a period of 3 hours. Behaviors are recorded from a top
817 view camera capturing the entire apparatus. Videos were scored using BORIS[124] post-
818 test by validated scorers blind to condition. Observed behaviors included location (i.e.,
819 duration of time in partner, stranger, and neutral chambers), duration of stationary
820 huddling or >50% side-by-side contact between the partner and stranger animals, and
821 frequency of aggressive behavior (i.e., lunges). Of note, analysis of partner preference
822 between wild type siblings from the $Oxtr^{1-/-}$ background and wild type animals from the
823 breeding colony showed no difference in time spent huddling with partner vs stranger
824 animals.
825
826 ***Bond maintenance assays***
827 Four days after the timed mating assay, female animals underwent a separation-
828 reunification assay. Females remained in their home cage while their male partners
829 were placed in a separate cage in another room for one hour. The males were then
830 reintroduced into the home cage and behavior was video recorded for 30 minutes. Male
831 subject animals underwent the same procedure five days following timed mating. Two
832 days following the separation reunification test, animals underwent a selective
833 aggression assay. Partners were again removed from the home cage and separated to

834 a separate room for an hour. After one hour, a novel sexually naïve animal of the
835 opposite sex was introduced into the home cage with the subject animal and behavior
836 observed for 20 minutes. If significant aggression occurred, defined as >3 tussles during
837 the assay, the animals were separated and the assay terminated. Overall, two WT
838 female assays and one $Oxtr^{1-/-}$ were terminated for aggression. The same behaviors
839 listed above for the introduction were observed and recorded in the reunification and
840 aggression assays.
841

842 **RNA Sequencing**

843 ***Sample collection***

844 Adult 7-9 week old WT and $Oxtr^{1-/-}$ voles were either cohoused with same sex-siblings or
845 paired with an animal of the opposite sex for four days following the timed mating protocol
846 described above. These animals were euthanized by CO_2 inhalation and decapitated. The
847 brain was quickly dissected out and sectioned into 500μm coronal slices using a brain
848 matrix mold (BrainTree Scientific) chilled on ice. Slices were floated in ice-cold phosphate
849 buffered saline (PBS), the NAc was identified using anatomical landmarks, and dissected
850 using a Zeiss microscope. A total of 45 WT females, 39 WT males, 21 $Oxtr^{1-/-}$ females,
851 and 18 $Oxtr^{1-/-}$ males were split between paired and unpaired conditions and tissue from
852 three animals per condition was pooled prior to RNA extraction. Tissue was flash-frozen
853 in liquid nitrogen and stored at -80°C until further processing. Total RNA was extracted
854 using TRIzol according to manufacturer's instructions and quantified using NanoDrop
855 (Thermo Scientific). Library preparation for next generation sequencing, comprising 35
856 samples and 4 technical replicates, was done using TruSeq Stranded mRNA Kit

857 according to manufacturer recommendations and sequenced on a NovaSeq 6000 to an
858 average depth of 2.9e07 reads per sample. Sequencing was performed across three
859 runs, but all data was processed together.
860
861 ***Read processing***
862 Adapter and low-quality sequence trimming was performed with Trimmomatic v0.39
863 using parameters: 'TruSeq3-PE.fa:2:30:10:2:keepBothReads LEADING:3 TRAILING:3
864 SLIDINGWINDOW:4:20 MINLEN:25' (Bolger et al., 2014). Trimmed RNA-Seq reads
865 were aligned to a custom MicOch1.0 prairie vole genome, which incorporated a known
866 missing gene V1A, using STAR v2.7.3a in gene annotation mode (Dobin et al., 2013).
867 Alignment, RNA-Seq, and Insert Size quality control metrics were generated using
868 Picard v 2.10.10 (http://broadinstitute.github.io/picard). Homologous genes between
869 vole, mouse, and human references were identified using biomart v2.56.1. When
870 multiple mouse or human genes mapped to the same vole gene, the homologous gene
871 with the highest percent identity to vole was selected.
872
873 ***Differential expression analysis***
874 To remove non- and lowly-expressed genes, only genes with more than 2 counts per
875 million (cpm) in at least 3 samples were retained. Principal component analysis of the
876 cpm revealed that technical replicates all cluster tightly but showed a slight batch effect
877 due to sequencing run (Fig. S5A). To remove this effect, we used RUVSeq v1.34.0 to
878 estimate one factor of unwanted variation, W_1, which we later used to normalize the
879 data prior to differential expression[125]. The factor analysis was performed on the

880 deviance residuals from an initial generalized linear model regression of the upper
881 quartile normalized counts on our covariates of interest (pair bonding status, genotype,
882 sex). Expressed genes were tested for differential expression (DE), after combining
883 technical replicates, with DESeq2 v1.40.2 using a design matrix that included the
884 covariates and W_1[126]. The adaptive shrinkage estimator ashr v2.2-63 was used in
885 order to be more robust to genes with low cpm values[127]. For DE analyses in general,
886 while most changes were driven by female samples, the effect was maintained in the
887 males at a smaller magnitude; thus, analyses were primarily performed for both sexes
888 jointly to maximize accuracy and power.
889
890 *Bonding effect*
891 To compare pre- to post-pairing individuals, we performed the DE analysis in two ways.
892 First, we compared pairing status regardless of genotype or sex to increase our
893 statistical power and to identify a reproducible gene set of thirteen genes (Fig. 5B, 5C,
894 S5B). While the relationship between the genes is unknown, there is support that the
895 proteins are functionally related. Using the STRING protein database
896 (STRINGdb_2.12.1), the human-homologs of the DE genes share more connections
897 than we would expect by chance (Fig. S5C, p-value= 3.08E-0.7). Next, we compared
898 pairing status using all three covariates, to identify subgroup-specific genes of interest
899 and effect sizes (Fig. 5D, S5D). In both analyses, genes were considered significantly
900 DE with a BH adjusted p-value < 0.05.
901

902 *Genotype effect*

903 To examine the effect of genotype, we first performed DE analyses between WT and
904 Oxtr$^{-/-}$ individuals, not including sex as a covariate to identify a reproducible and
905 stringent gene set. We considered genes DE with an adjusted p-value < 0.05 and
906 absolute log2 fold-change > 0.25 (Fig. 6B, S6A, S6B). To examine the functional
907 relationship of the DE genes, we performed a Gene Ontology enrichment analysis using
908 goseq v1.52.0 which controls for gene length bias[128]. We considered all expressed vole
909 genes with a mouse homolog as our background and all DE genes with a mouse
910 homolog as our foreground. GO categories with an adjusted p-value < 0.05 were
911 considered significantly enriched. To help visualize the results, enriched GO categories
912 were clustered according to their semantic similarity calculated with the R package
913 GOSemSim v2.26.1 using method "Wang"[129]. Large, general, GO categories with over
914 1000 genes were excluded in visualizations (Fig. 6C). WikiPathways[130] over-
915 representation analysis was performed with R package clusterProfiler v4.8.3[131] (Fig.
916 S6D).

917

918 For disorder and disease set overrepresentation analysis, Chi-squared tests were used
919 to assess whether Oxtr$^{1-/-}$ disrupted genes occur in disease-associated gene lists at a
920 frequency higher than we would expect by chance. Genes lists for autism spectrum
921 disorder[74], schizophrenia[75], neurodevelopmental disorders[77], and epilepsy[76] were
922 sourced and all alternate or outdated gene symbols were updated manually. For this
923 test, we were interested in sex- and direction-specific enrichments, so we performed a
924 DE analysis separately for males and females. Across all DE analyses, we defined DE

925 genes more stringently (adjusted p-value < 0.01). For enrichment tests, our universe
926 was all expressed vole genes with a human homolog. We split this analysis by fold-
927 change direction to highlight the distinct enrichment in upregulated genes. P-values
928 underwent BH correction across all 24 comparisons.
929
930 To compare to mouse neuronal populations, we leveraged single-cell data on mouse
931 hypothalamus development[83]. The released Seurat object
932 GSE132730_subset_cca_to_velo.rds.gz was accessed at GSE132730. Using the
933 authors' defined clusters (accessed at "prim_walktrap"), we assessed how similar each
934 clusters' gene expression is to the genes disrupted by the $Oxtr^{1-/-}$ mutation. This was
935 calculated as the Jaccard similarity coefficient using R package clustifyR v1.12.0[132].
936
937 ***Weighted Gene Coexpression Network Analysis***
938 Data
939 Starting with the RNAseq dataset of n=30 samples (one WT sample and 4 replicate
940 samples were removed) and n=13357 genes, we removed genes with low expression
941 (n=1738 genes with expression level in lowest quantile for all 30 samples) and/or low
942 variability (n=8230 genes with coefficient of variation < 0.05), resulting in a trimmed
943 dataset of n=3389 genes.
944
945 Identifying co-expression modules
946 We used the R package WGCNA (v1.70-3) to conduct WGCNA analyses[72]. Briefly, we
947 calculated Pearson correlations for all gene pairs. Next, we constructed an unsigned

948 weighted correlation network to identify co-expression modules comprised of highly
949 correlated genes (positive or negative correlation) with high topological overlap[133].
950 Modules were defined as branches of a hierarchical cluster tree using the top-down
951 dynamic tree cut method[72]. For each module, the expression pattern was summarized
952 by the module eigengene (ME), which is defined as the right singular vector of the
953 expression patterns. Pairs of modules with high module eigengene correlations ($r >$
954 0.75) were merged to maintain a level of decorrelation among MEs.
955
956 In more detail, a weighted unsigned network was computed based on a fit to scale-free
957 topology, and the lowest thresholding power that resulted in a scale-free R^2 fit of 0.9
958 was selected, and the pairwise topological overlap (TO) between genes was
959 calculated[133] . We constructed a TO dendrogram using hierarchical clustering (R::hclust
960 function, method= ”average”), and defined modules using the WGCNA::cutreeHybrid
961 function with minimum module size set to 30 genes. We then merged modules with high
962 module eigengene correlations as describe above.
963
964 We calculated 3 sets of modules from different sample subsets:
965 1. $Modules^{WT}$: n=15 modules constructed from n=18 WT samples with
966 thresholding power $\beta = 5$.
967 2. $Modules^{Mut}$: n= 43 modules constructed from n=12 $Oxtr^1$-mutant samples
968 with thresholding power $\beta = 6$.
969 3. $Modules^{All}$: n=7 modules constructed from all n=30 samples with
970 thresholding power $\beta = 3$

971

972 Relating modules to sample traits

973 In order to correlate modules with experimental conditions, we calculated the Pearson
974 correlations between module eigengenes and sample metrics, including species
975 (Mut=0, WT=1), condition (Pre=1, Post=0), sex (F=1, M=0), and quality control (QC)
976 metrics (RIN, yield, sequencing run). We identified three modules that significantly
977 correlated with a sample metric of interest but not with any of the QC metrics.
978 Significant correlation was defined to be $p_{adj} <= 0.05$, where p_{adj} = BH correction by
979 number of modules. These modules (M) were:

980 1. $Mpink^{WT}$: positive correlation with pre-bonding status (Pearson R = 0.7, p_{adj} =
981 0.018)
982 2. $Mbrown^{All}$: positive correlation with WT status (Pearson R = 0.55 , p_{adj} = 0.011)
983 3. $Mturquoise^{All}$: positive correlation with WT status (Pearson R = 0.8, p_{adj} = 6.6e-7)

984 We calculated the module eigengenes (ME) for $Mpink^{WT}$, $Mbrown^{All}$, and $Mturquoise^{All}$
985 for all n=30 samples using the WGCNA::moduleEigengenes function. We then
986 conducted Wilcoxon rank sum tests (ggpubr::stat_compare_means function) to assess
987 whether MEs were significantly different between the following groups:

988 1. $MEpink^{WT}$: pre- versus post-bonded animals, separated by sex and species
989 2. $Mbrown^{All}$: WT versus mutant animals, separated by sex and condition
990 3. $Mturquoise^{All}$: WT versus mutant animals, separated by sex and condition

991

992 Comparing gene significance with module membership:

993 We assessed whether genes whose expression highly correlate with module
994 eigengenes of modules of interest ($Mpink^{WT}$, $Mbrown^{All}$, and $Mturquoise^{All}$) are
995 themselves highly correlated with traits of interest (bonding status or mutation status).
996 Specifically, for the genes in $Mpink^{WT}$, $Mbrown^{All}$, and $Mturquoise^{All}$, we calculated 1)
997 gene significance (GS), defined as the absolute Pearson's correlation between
998 expression of a given gene and a trait of interest; and 2) module membership (MM),
999 which is defined as the absolute Pearson's correlation between the expression profile of
1000 a gene with the ME of a module to quantify the relationship between a gene and a given
1001 module[72]. We then calculated the Pearson correlations between:

1002 1. $GS^{condition}$ and $MMpink^{WT}$ for $Mpink^{WT}$ genes (R = 0.69, p = 5.5e-18)
1003 2. $GS^{species}$ and $MMbrown^{All}$ for $Mbrown^{All}$ genes (R = 0.63, p = 2.2e-32)
1004 3. $GS^{species}$ and $MMturquoise^{All}$ for $MMturquoise^{All}$ genes (R= 0.82, p<1e-200)

1005 Hub genes were defined as those genes in the top 25% for both the absolute value of
1006 pink module membership and the absolute value of correlation with bonding status.
1007

1008 <u>Assessing whether modules are enriched for DE genes</u>

1009 We were interested in assessing whether $Mpink^{WT}$ genes are significantly enriched for
1010 any the DE pre vs post pairing gene set described above. We assessed for enrichment
1011 of DE gene sets using a hypergeometric test.
1012

1013 <u>WT module preservation analysis (Zsummary)</u>

1014 We assessed how well $modules^{WT}$ are preserved in mutant samples. We calculated a
1015 $Z_{summary}$ statistic for each $module^{WT}$ [134] using the WGCNA::modulePreservation function

1016 with 200 permutations. The $Z_{summary}$ measure combines module density and
1017 intramodular connectivity metrics to a composite statistic where Z>2 suggests moderate
1018 preservation and Z>10 suggests high preservation. We found of all the n=15
1019 modules^{WT}, Mpink^{WT} had the lowest $Z_{summary}$ ($Z_{summary}$=2) in mutant samples.
1020

1021 **Histology**

1022 ***Immunohistochemistry (IHC)***

1023 Sexually naïve voles group housed by sex after weaning (P0, P21, adults:10 - 14 weeks
1024 old), were perfused with 25mL ice cold phosphate buffer (PBS) and fixed in 25mL of 4%
1025 paraformaldehyde in PBS (PFA). Whole brain was dissected and post fixed overnight at
1026 4°C in 4% PFA in the dark. The tissue was cryoprotected for 24 hours in 30% sucrose in
1027 PBS and then embedded in OCT over dry ice to prevent cracking. 60µm serial sections
1028 from the entire PVN were collected in PBS and processed as free-floating sections.
1029 Sections were blocked using 10% donkey serum in 0.1% Triton X 100 in PBS and then
1030 stained with primary antibodies (Oxytocin Polyclonal Antibody, Invitrogen, Rabbit
1031 Polyclonal, Cat #PA5-26701, 1:1000 and Anti-Neurophysin 2/NP-AVP Antibody, clone
1032 PS 41, Millipore Sigma, Mouse Monoclonal, Cat#MABN845, 1:10,000) in 1% donkey
1033 serum with 0.1% Triton X 100 (staining buffer) in PBS at 4°C with shaking. The sections
1034 were rinsed and soaked in secondary antibodies (Cy™3 AffiniPure Donkey Anti-Rabbit
1035 IgG, Jackson ImmunoResearch Laboratory, Cat #711-165-152, 1:500 and Alexa Flour
1036 488 Donkey Anti Mouse IgG, Thermo Fisher Scientific, Cat #A21202, 1:500) in staining
1037 buffer for 2 hours at room temperature. Sections were DAPI stained and transferred to
1038 glass slides in sequence and mounted in Aquamount. Slides were imaged using a

1039 confocal microscope (Zeiss LSM 700) and the zstacks were quantified (cell count by
1040 hand and area hand selected and measured) in ImageJ. Comparisons of cell density
1041 (count/area) were made in age and sex matched samples.
1042

1043 ***In situ hybridization (ISH)***

1044 ISH was performed using RNA probes prepared as described previously[135], to detect
1045 expression of *Calcr, Dlk1*, and *Dgkb* mRNA in the adult vole brain. We prepared RNA
1046 sense and anti-sense probes corresponding to 706bp (CalcR), 773bp (Dgkb), and
1047 796bp (Dlk1) for genes of interest identified in the WT vs Oxtr DEX list from our RNAseq
1048 data. For ISH on adult animals, 7-9 week old WT and $Oxtr^{1-/-}$ voles of both sexes were
1049 either group housed with same sex conspecifics or paired for 4 days with a WT animal
1050 of the opposite sex following the timed mating protocol described above. The brains
1051 were processed as described for IHC, then embedded in OCT and sectioned at 50µm,
1052 mounted immediately after sectioning onto SuperFrost Plus glass microscope slides
1053 and stored at -80°C until ISH staining. Slides were fixed in 4% PFA for 20 minutes,
1054 rinsed in PBS, treated with proteinase K (10µg/mL, Roche) for 20 minutes, rinsed in
1055 PBS, and fixed again in 4% PFA for 5 minutes at room temperature. Slides were
1056 acylated for 10 mins then rinsed in 1% Triton100X in PBS followed by PBS. The slides
1057 were equilibrated in warm hybridization solution for 1-2 hours at 65°C and subsequently
1058 incubated with a temporary paraffin cover for 14 - 18 hours at 65°C in fresh
1059 hybridization buffer containing RNA probe. After incubation, the slides were dipped in
1060 5X SSC warmed to 72°C to remove the parafilm coverslips and then washed in 0.2X
1061 SSC warmed to 72°C. The slides were blocked with 10% heat inactivated sheep serum

1062 (HISS) solution then stained for 12 - 18 hours at 4°C in buffer containing 10% HISS and
1063 alkaline phosphatase-conjugated sheep anti- digoxigenin antibody (1:2000, Roche).
1064 After extensive washing, the slides were incubated for ~72 hours at 37°C in staining
1065 solution containing nitro blue tetrazolium and 5- bromo-4-chloro-3-indolyl-phosphate
1066 (Roche). The slides were finally washed, fixed in 4% PFA, and coverslipped. Slides
1067 were imaged using a Keyence fluorescence microscope and the z-stacks were
1068 quantified (cell count and area) in ImageJ. For signal quantitation, positive puncta were
1069 counted in every third coronal section encompassing the entire anterior to posterior
1070 gene expression domain. Cell counts were normalized by total area for a gene
1071 expression domain in each section. Positive signal was quantified by calculating total
1072 area of signal multiplied by the average intensity of signal (total area x mean pixel
1073 intensity) in gene expression domains of a section; every third section was quantified
1074 and added. Comparisons of cell counts were made in age and sex matched samples.

1075 **Quantification and Behavioral Analysis**

1076 For detailed statistical methods please see Table S1. The number of animals used was
1077 based on previous studies in the field by our group and others, combined with a power
1078 analysis. Assumptions of independence and normality were considered with multiple
1079 tests. Preference index (PI) was calculated as (partner huddle duration – stranger huddle
1080 duration)/(partner huddle duration + stranger huddle duration). Sliding partner preference
1081 was calculated by calculating PI for a single animal in 20-minute intervals where each
1082 interval overlapped the next by 15 minutes (e.g. 0-20mins, 5-25mins…). To look at
1083 convergence in sliding PI the area under the curve (Area above 0 – Area below 0, AUC)
1084 for each hour of the assay was determined for each animal and then pooled for each

choosing animal by sex and then condition. Preference was determined as significantly convergent if the AUC from the hour of assay for all animals within the group significantly differed from 0 using a One sample t Test. The level of statistical significance for each test was set at $p =< 0.05$. Outliers were detected using a combination of z-score (+/- 3) and plots of original and log-transformed data. Analyses were completed in RStudio (version 2024.04.2+764) and GraphPad Prism (version 10.3.1)

1091 **FIGURE LEGENDS**

Figure 1: Oxtr reduces the amount of time naïve animals take to show partner preference

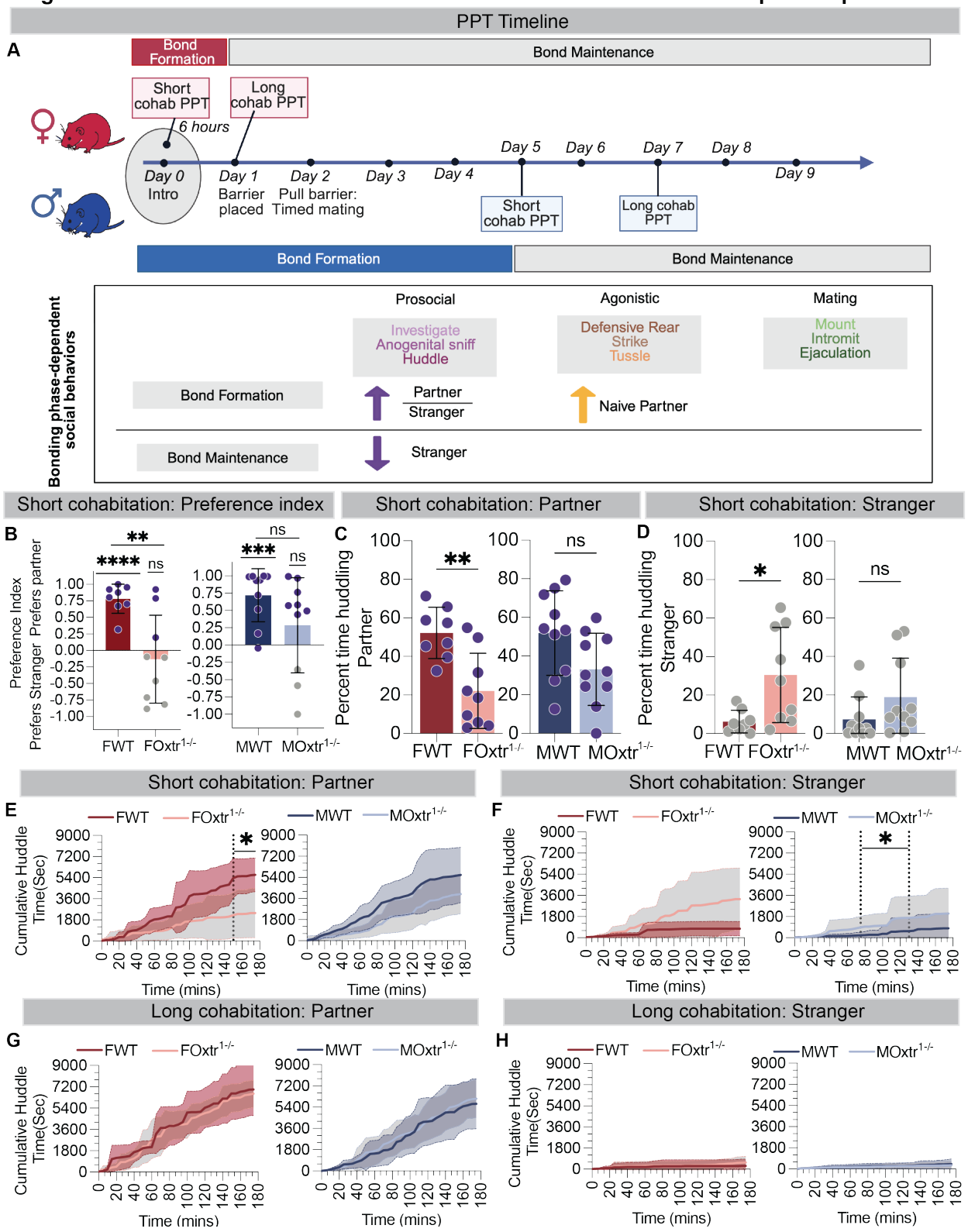

1092

1093 **Figure1: Oxtr reduces the amount of time naive animals take to show partner**
1094 **preference**

1095 A. Schematic of the partner preference tests (PPTs) and the day on which they were
1096 conducted to study pair bonding behaviors. The prosocial, agonistic and mating
1097 behaviors scored are shown below. During the bond formation phase, the ratio of
1098 partner-directed vs stranger-directed affiliative behaviors increases in wild types
1099 and following the bond formation in the bond maintenance phase, wild types show
1100 decreased prosocial behaviors and increased agonistic behaviors towards
1101 strangers.

1102 B. A preference for partner is induced in the WTs but not $Oxtr^{1-/-}$ animals following
1103 short cohabitation.

1104 C. WT females spend more time huddling with their partners.

1105 D. $Oxtr^{1-/-}$ females spend more time huddling with strangers.

1106 E. WT females show a significant increase in partner huddling time towards the end
1107 of a 3-hour assay.

1108 F. $Oxtr^{1-/-}$ males show a significant increase in stranger huddling time in the middle of
1109 a 3-hour assay.

1110 G. No difference in partner huddling time between WT and $Oxtr^{1-/-}$ animals following
1111 long cohabitation.

1112 H. No difference in stranger huddling time between WT and $Oxtr^{1-/-}$ animals following
1113 long cohabitation.

1114 See Supplementary Figure 1 and Supplementary Table 1.

1115 Mean +/- SD, n =>8, *p =< 0.05, FWT = female WT, FOxtr$^{1-/-}$ = female Oxtr$^{1-/-}$, MWT =

1116 male WT, MOxtr$^{1-/-}$ = male Oxtr$^{1-/-}$.

Figure 2: Oxtr suppresses promiscuous behaviors in a state dependent manner in females

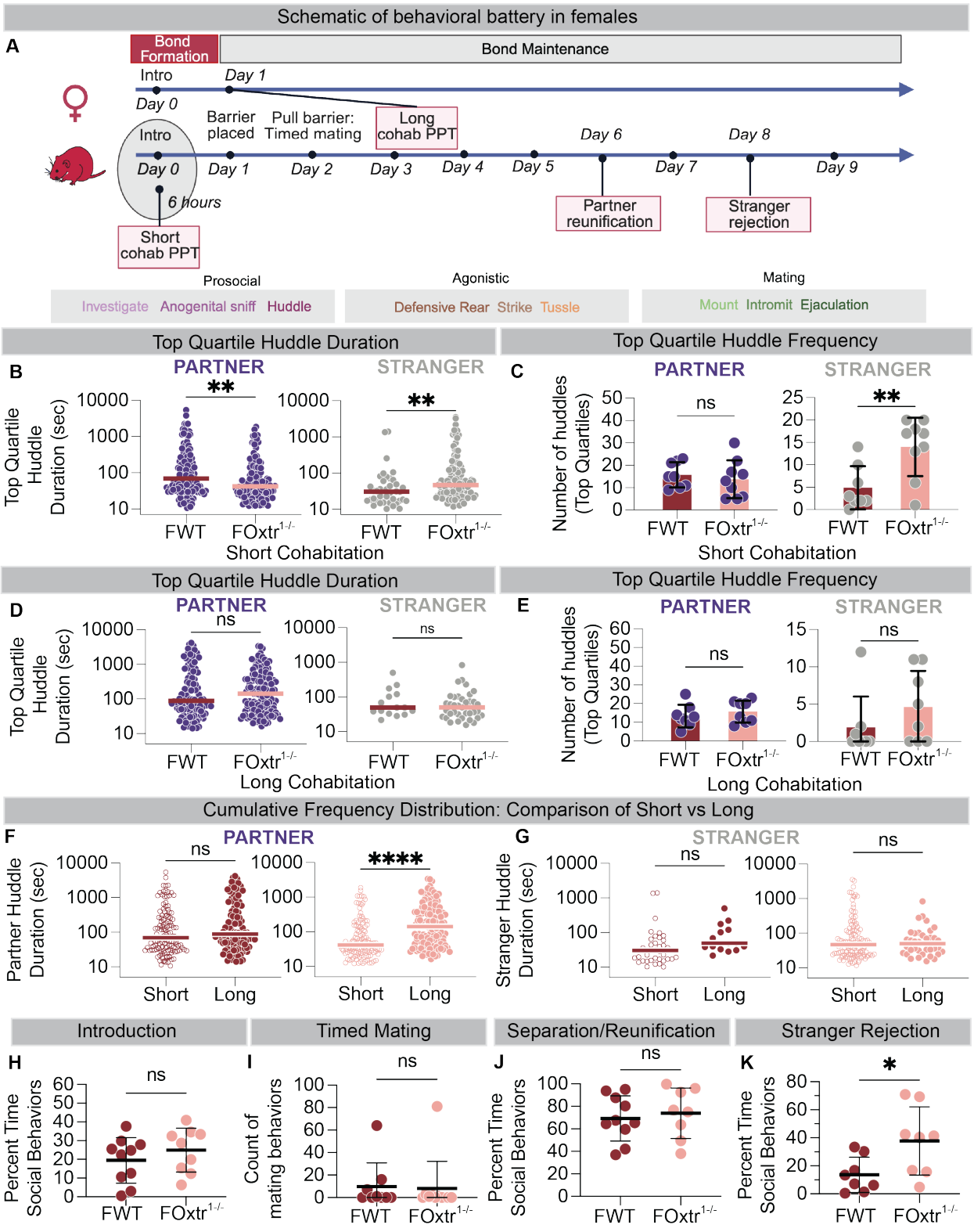

1119 **Figure2: Oxtr suppresses promiscuous behaviors in a state dependent manner in**
1120 **females**

1121 A. Timeline of the behavioral battery carried out on females. Bottom row shows the
1122 behaviors scored.
1123 B. Oxtr$^{1-/-}$ female long huddle duration is shorter with partners and longer with
1124 strangers after a short cohabitation.
1125 C. Oxtr$^{1-/-}$ female long huddle frequency is greater with strangers, but not partners
1126 after a short cohabitation.
1127 D. No difference in median long huddle durations between WT and Oxtr$^{1-/-}$ females
1128 post long cohabitation.
1129 E. No difference in long huddle frequencies between WT and Oxtr$^{1-/-}$ females post
1130 long cohabitation.
1131 F. Increasing cohabitation time increases the median long huddle duration an Oxtr$^{1-/-}$
1132 female executes with the partner.
1133 G. There is no significant change in the median long huddle duration conducted by
1134 females with strangers when cohabitation time is increased.
1135 H. Naive Oxtr$^{1-/-}$ and WT females are equally prosocial towards a naive WT male.
1136 I. There is no difference in the counts of mating behaviors between Oxtr$^{1-/-}$ and WT
1137 females.
1138 J. Oxtr$^{1-/-}$ and WT females are equally prosocial towards their partners after a brief
1139 separation.
1140 K. Oxtr$^{1-/-}$ females are significantly more prosocial towards a naive WT stranger male
1141 compared to WT females.

1142 See Supplementary Figure 2 and Supplementary Table 1.

1143 Mean ± SD, n =>8, *$p < 0.05$, FWT = female WT, FOxtr$^{1-/-}$ = female Oxtr$^{1-/-}$, MWT = male

1144 WT, MOxtr$^{1-/-}$ = male Oxtr$^{1-/-}$.

Figure 3: Oxtr function influences different prosocial behaviors across pair bonding in males

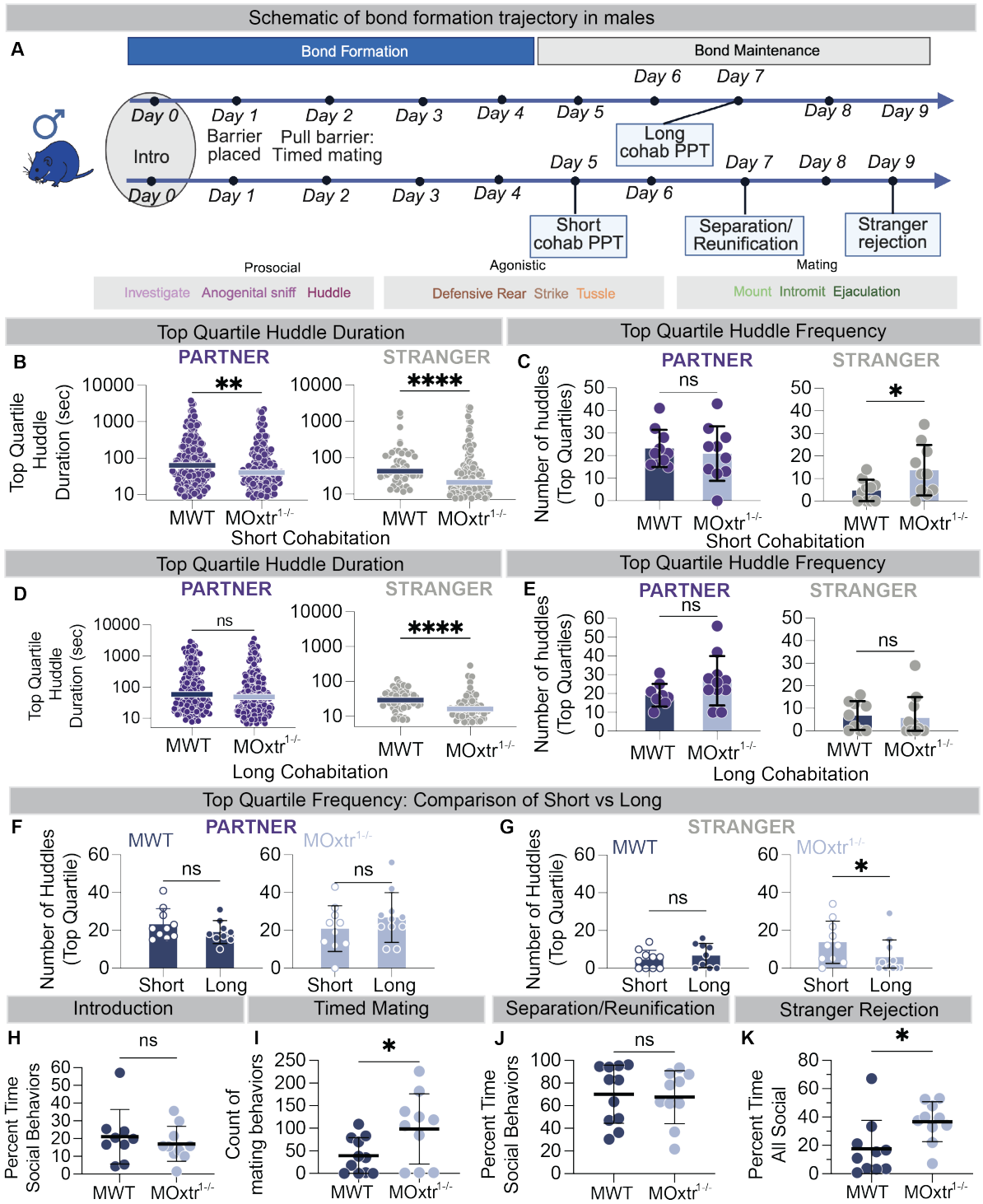

Figure3: Oxtr function influences different prosocial behaviors across pair bonding in males

1148 A. Timeline of the behavioral battery carried out on males. Bottom row shows the
1149 behaviors scored.
1150 B. $Oxtr^{1-/-}$ male long huddle duration is shorter with partners and strangers after a
1151 short cohabitation.
1152 C. $Oxtr^{1-/-}$ male long huddle frequency is greater with strangers, but not partners after
1153 a short cohabitation.
1154 D. The median long huddle executed by $Oxtr^{1-/-}$ males with the stranger after a long
1155 cohabitation, is shorter than their WT siblings.
1156 E. No difference in the long huddle frequencies between WT and $Oxtr^{1-/-}$ males post
1157 long cohabitation.
1158 F. There is no change in the frequency of long huddles with partner between $Oxtr^{1-/-}$
1159 and WT males.
1160 G. Increasing cohabitation time decreases the frequency of long huddles with
1161 strangers in $Oxtr^{1-/-}$ males.
1162 H. Naive $Oxtr^{1-/-}$ and WT males are equally prosocial towards naive WT females.
1163 I. $Oxtr^{1-/-}$ males execute higher counts of mating behaviors compared to WT.
1164 J. Prosocial behaviors following a brief separation with their partner are not different
1165 between $Oxtr^{1-/-}$ and WT males.
1166 K. $Oxtr^{1-/-}$ males are significantly more prosocial towards a naive WT stranger female
1167 compared to WT males.
1168 See Supplementary Figure 3 and Supplementary Table 1.
1169 Mean +/- SD, n =>8, *p =< 0.05, FWT = female WT, $FOxtr^{1-/-}$ = female $Oxtr^{1-/-}$, MWT =
1170 male WT, $MOxtr^{1-/-}$ = male $Oxtr^{1-/-}$

Figure 4: Oxtr sex-specifically influences social interactions between potential mates

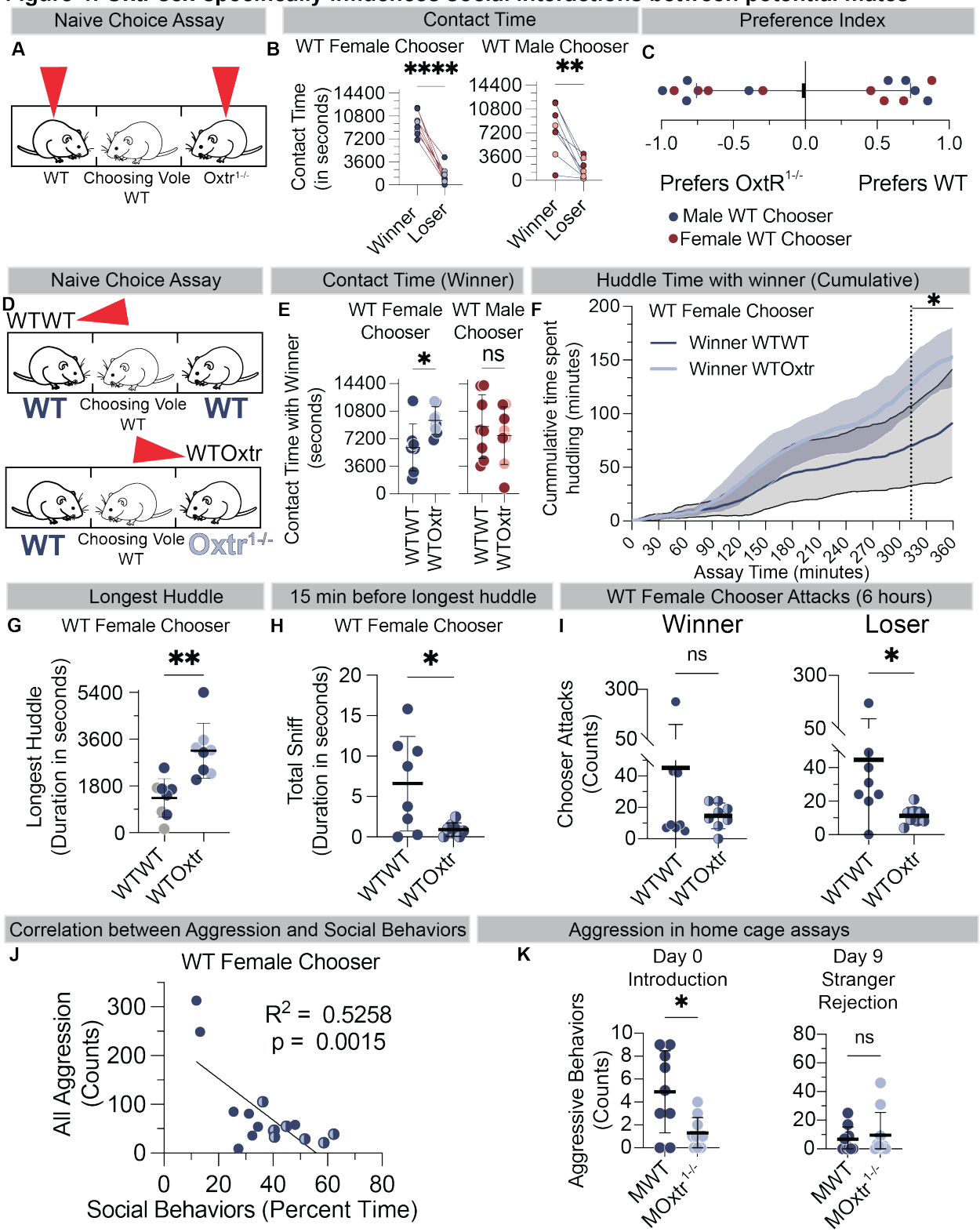

1171

1172 **Figure4: Oxtr sex-specifically influences social interactions between potential**
1173 **mates**

1174 A. Schematic of naive social choice with a naive WT animal choosing between an
1175 opposite sex WT and opposite sex $Oxtr^{1-/-}$ animal (red triangles).
1176 B. WT choosers of both sexes spend significantly more time with one stimulus
1177 animal (winner) over the other (loser). The color of each dot denotes the
1178 genotype of the winner and loser.
1179 C. WT and $Oxtr^{1-/-}$ animals are chosen as winners with equal frequency by WT
1180 choosers of both sexes.
1181 D. Schematic of comparison of contact with winner from WTOxtr condition to that
1182 with winner from WTWT condition.
1183 E. Female WT choosers spends more time in contact with a winner from a WTOxtr
1184 condition than the WTWT. The color of the dots represents the genotype of the
1185 winner.
1186 F. Female WT choosers spend significantly more time huddling with the winner from
1187 the WTOxtr condition in the last 47 mins of the assay. Solid lines depict the
1188 average cumulative huddle time, the solid black bar denotes the time at which
1189 the lines significantly diverge.
1190 G. Longest huddle from WTOxtr lanes is significantly higher compared to those from
1191 WTWT lanes. The color of each dot denotes the genotype/position of the animal
1192 with whom the longest huddle took place.

1193 H. Female WT choosers from WTWT lanes spend more time sniffing both stimulus
1194 animals 15 minutes before the longest huddle compared to female choosers from
1195 WTOxtr lanes
1196 I. Female WT choosers attack the loser in WTWT lanes more frequently than
1197 choosers from WTOxtr lanes (right). There is no difference in the number of
1198 attacks on the winners by female choosers from WTWT lanes compared to those
1199 from WTOxtr lanes (left).
1200 J. Total prosocial behavior time shows significant negative correlation with the total
1201 counts of aggressive behaviors displayed by female WT choosers.
1202 K. Naive male WTs attack a potential female WT mate more frequently than male
1203 $Oxtr^{1-/-}$ animals (left). There is no difference in the number of attacks against an
1204 unfamiliar naive WT female stranger by bonded WT and $Oxtr^{1-/-}$ males (right).

1205 See Supplementary Figure 4 and Supplementary Table 1.

1206 Mean +/- SD, n = 8, *p =< 0.05, FWT = female WT, $FOxtr^{1-/-}$ = female $Oxtr^{1-/-}$, MWT = male
1207 WT, $MOxtr^{1-/-}$ = male $Oxtr^{1-/-}$, WTWT = Lane with 2 naive WT animals, WTOxtr = Lane with
1208 a WT and a $Oxtr^{1-/-}$ animal.

Figure 5: Post pair bonding gene expression is driven by female specific changes dependent on Oxtr signaling

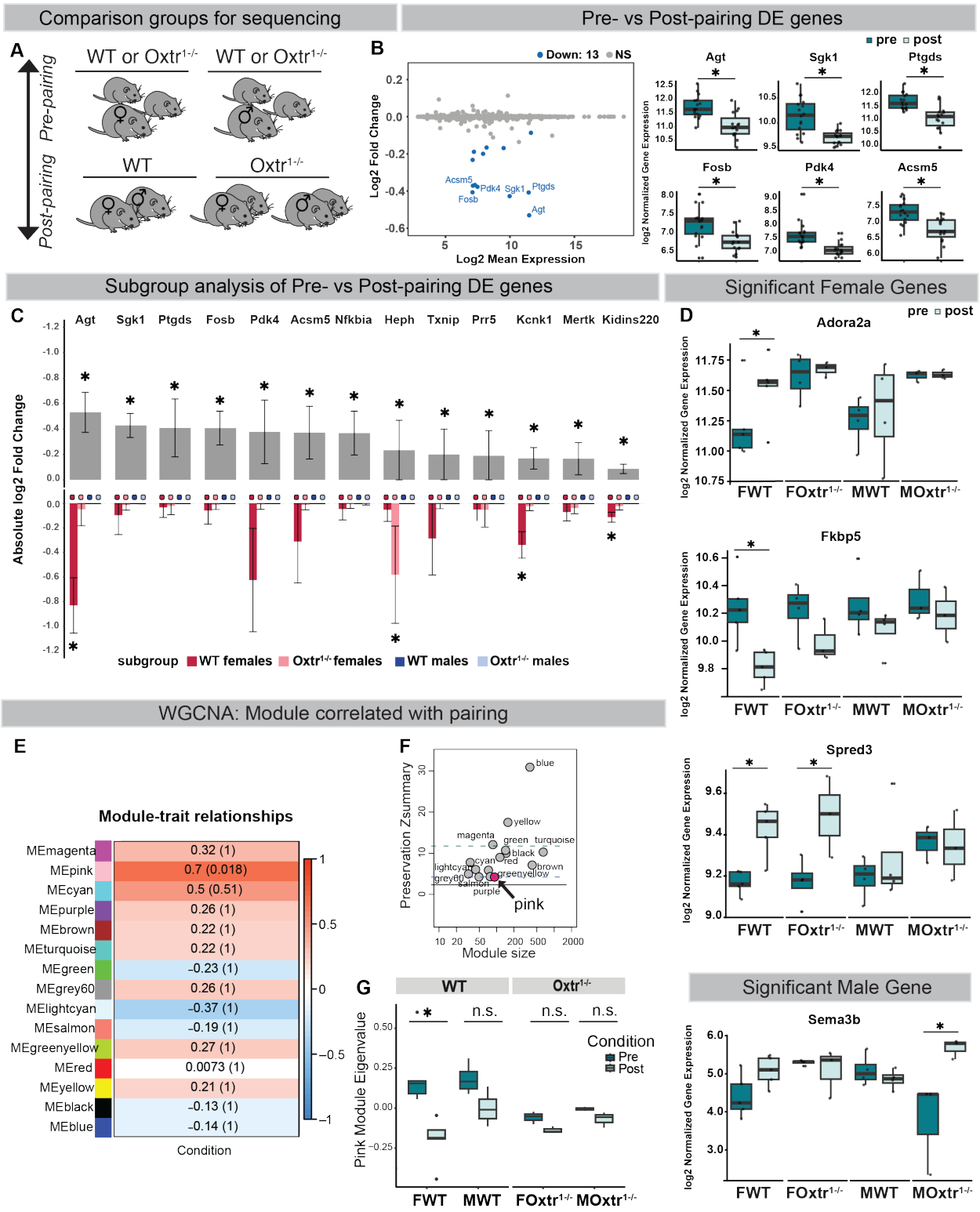

1209

1210 **Figure 5: Post pair bonding gene expression is driven by female specific changes**
1211 **dependent on Oxtr signaling**

1212 A. Schematic of experimental groups used for sequencing highlighting pre- vs post-
1213 pairing comparisons between groups. Animals with symbols represent those used
1214 for tissue collection.

1215 B. Scatterplot illustrating the relationship between fold change and mean expression,
1216 emphasizing the 13 differentially expressed (DE) genes in post-pairing individuals
1217 compared to pre-pairing. Gray dots indicate non-significant genes ($p_{adj} > 0.05$);
1218 Blue dots indicate downregulated genes ($p_{adj} < 0.05$, $log_2FC < 0$) and upregulated
1219 genes in red ($p_{adj} < 0.05$, $log_2FC > 0$). The right panel shows box plots of normalized
1220 gene expression for the top six DE genes by fold-change between pre- and post-
1221 pairing conditions.

1222 C. Bar graph emphasizing how each combination of genotype and sex (denoted at
1223 bottom as 'subgroup') influence the 13 overall pairing-DE genes identified. The top
1224 graph depicts the absolute fold change and standard error of the differential
1225 expression analysis including all pre- and post-bonding individuals in which the 13
1226 genes of the x axis were identified. The bottom graph depicts the absolute fold
1227 change and standard error in analyses when only individuals of that subgroup were
1228 considered. (* denotes $p_{adj} < 0.05$ for the pre- vs post-pairing analysis).

1229 D. Box plots of select genes that show sex- and genotype-specific changes in
1230 expression with pairing condition. *Adora2A* and *Fkbp5* are DE when considering
1231 WT females, *Spred3* is DE when considering WT and $Oxtr^{1-/-}$ females, and *Sema3b*
1232 is DE when considering $Oxtr^{1-/-}$ males. Note: Sema3b is the mouse ortholog gene

1233 symbol for vole gene “ENSMOCG00000019704” which does not have an assigned
1234 gene symbol.

1235 E. Heatmap showing correlations between module eigengenes (MEs) for modules^{WT}
1236 and pairing condition (Pre=1, Post=0). Heatmap color and value reflect Pearson
1237 correlation coefficient; adjusted p values shown in parentheses (p_{adj} = p * number
1238 of modules).

1239 F. Preservation of modules^{WT} in OXTR-mutant samples. The $Z_{summary}$ measure
1240 combines module density and intramodular connectivity metrics to a composite
1241 statistic where Z>2 suggests moderate preservation and Z>10 suggests high
1242 preservation[134]. Of all modules^{WT}(n=15), Mpink^{WT} had the lowest $Z_{summary}$
1243 ($Z_{summary}$=2) in mutant samples.

1244 G. Box plots showing comparison of MEpink^{WT} for pre- vs post-pairing condition
1245 separated by sex and genotype. (Wilcoxon rank sum test, Bonferroni adjusted for
1246 4 comparisons).

1247 For all box plots center = median, box boundaries = 1st and 3rd quartile, whiskers =
1248 1.5*IQR from boundaries. (*n* = 16 pre-pairing and 15 post-pairing)

1249 See Supplementary Figure 5.

Figure 6: Oxtr regulated genes are common to social behavior relevant processes across species and are similarly regulated across brain regions

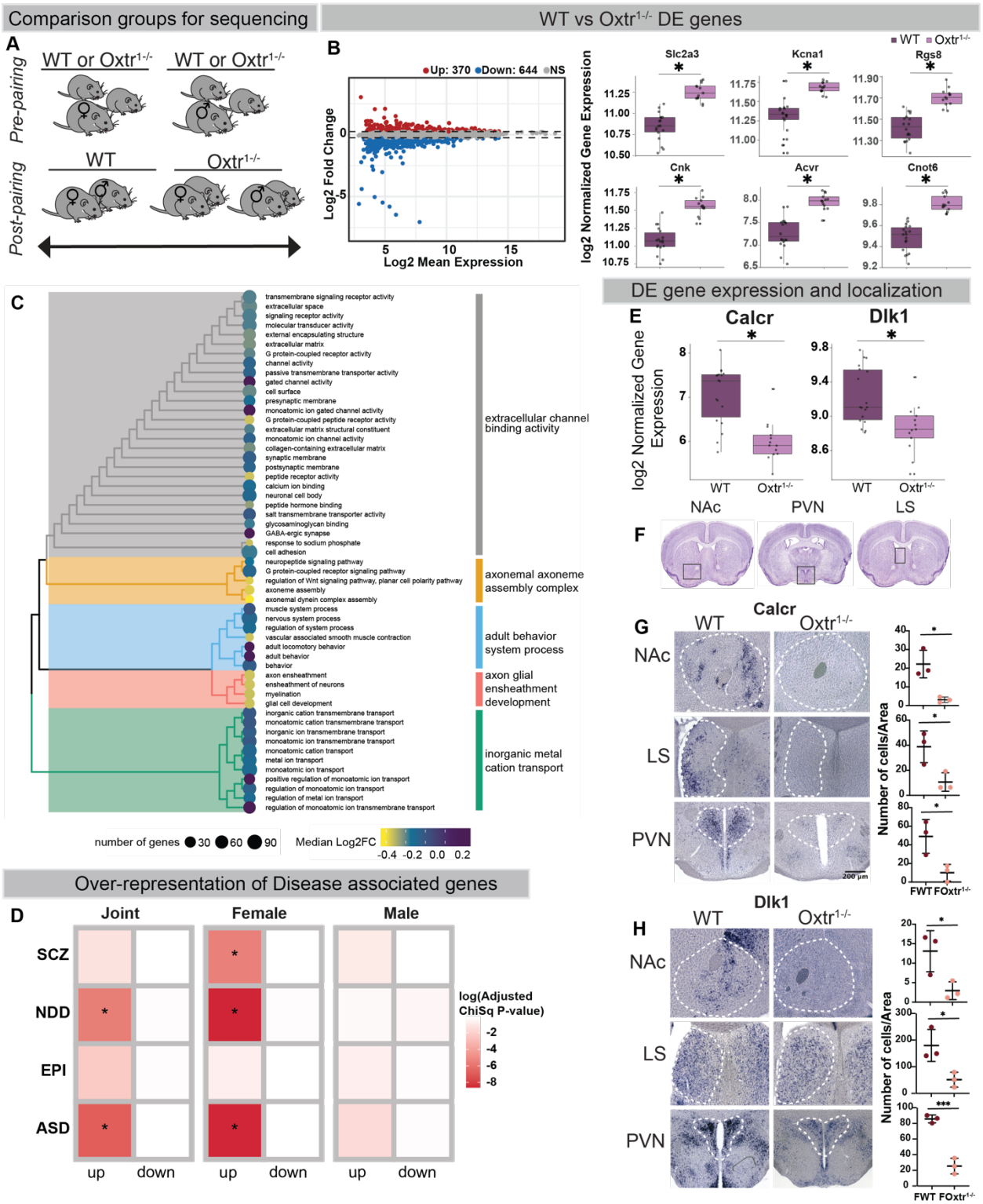

1250

1251 **Figure 6: Oxtr regulated genes are common to social behavior relevant processes**
1252 **across species and are similarly regulated across brain regions**

1253 A. Schematic of experimental groups for sequencing, highlighting genotype
1254 comparisons between groups. Animals with symbols represent those used for
1255 tissue collection.

1256 B. Scatterplot illustrating the relationship between fold change and mean expression,
1257 emphasizing differentially expressed (DE) genes in $Oxtr^{1-/-}$ individuals compared
1258 to WT. Significantly downregulated genes are shown in blue ($log_2FC<-0.25$,
1259 $p_{adj}<0.05$) and upregulated genes in red ($log_2FC>0.25$, $p_{adj} < 0.05$). Box plots of
1260 normalized gene expression for the top six DE genes by fold change between
1261 genotypes.

1262 C. Gene Ontology enrichment analysis for all genotype-DE genes (n=1014) highlights
1263 processes related to extracellular channel binding activity, axonal processes,
1264 behavior related gene expression, and cation transport. The leaves represent
1265 significant GO categories (BH adjusted p value < 0.05) which have been
1266 hierarchically clustered by their semantic similarity. Branches are colored by
1267 cluster and high-frequency words are displayed to the right. Leaf size and color
1268 correspond to the number and median fold change of DE genes in each category.

1269 D. Enrichment analysis shows that genes which are DE in $Oxtr^{1-/-}$ samples are over-
1270 represented in some neuropsychiatric disease-associated gene sets. The first DE
1271 gene set evaluated ('Joint') represents genes which are DE in $Oxtr^{1-/-}$ samples
1272 when considering both sexes in the differential expression analysis ($p_{adj} < 0.01$).
1273 The second gene set are DE genes when only considering females, and the third

1274 when only considering males. Gene sets are further separated by direction of effect
1275 across the x-axis to highlight the enrichment in upregulated DE genes. Colors
1276 correspond to the Benjamini-Hochberg corrected Chi-square p values; asterisks
1277 denote $p_{adj} < 0.05$. Y-axis abbreviations are as follows: SCZ=schizophrenia,
1278 NDD=neurodevelopmental disorder, EPI=epilepsy, and ASD=autism spectrum
1279 disorder.

1280 E. Box plots of *Calcr* and *dlk1* normalized gene counts by genotype. Log_2FC:-0.962
1281 and p_{adj}: 1.75e-06 for *Calcr* and log_2FC: -0.276 and p_{adj}: 0.00334 for *dlk1* from
1282 comparison considering all WT and $Oxtr^{1-/-}$ samples.

1283 F. Brain regions selected for in situ analysis. (NAc=nucleus accumbens,
1284 PVN=paraventricular nucleus of the hypothalamus, LS=lateral septum)

1285 G. ISH images and quantification for *Calcr* expression in NAc, PVN, and LS from WT
1286 and $Oxtr^{1-/-}$ animals.

1287 H. ISH images and quantification for *Dlk-1* expression in NAc, PVN, and LS from WT
1288 and $Oxtr^{1-/-}$ animals.

1289 Box plots in G. and H. show comparison of the area-normalized cell number by
1290 genotype. (*n*=3 per condition, Wilcoxon sign rank, *=p<0.05, ***=p<0.001)

1291 See Supplementary Figure 6 and Supplementary Table 1.

Figure 7: Loss of Oxtr results in the decrease in density of Oxt and Avp expressing neurons in the PVN

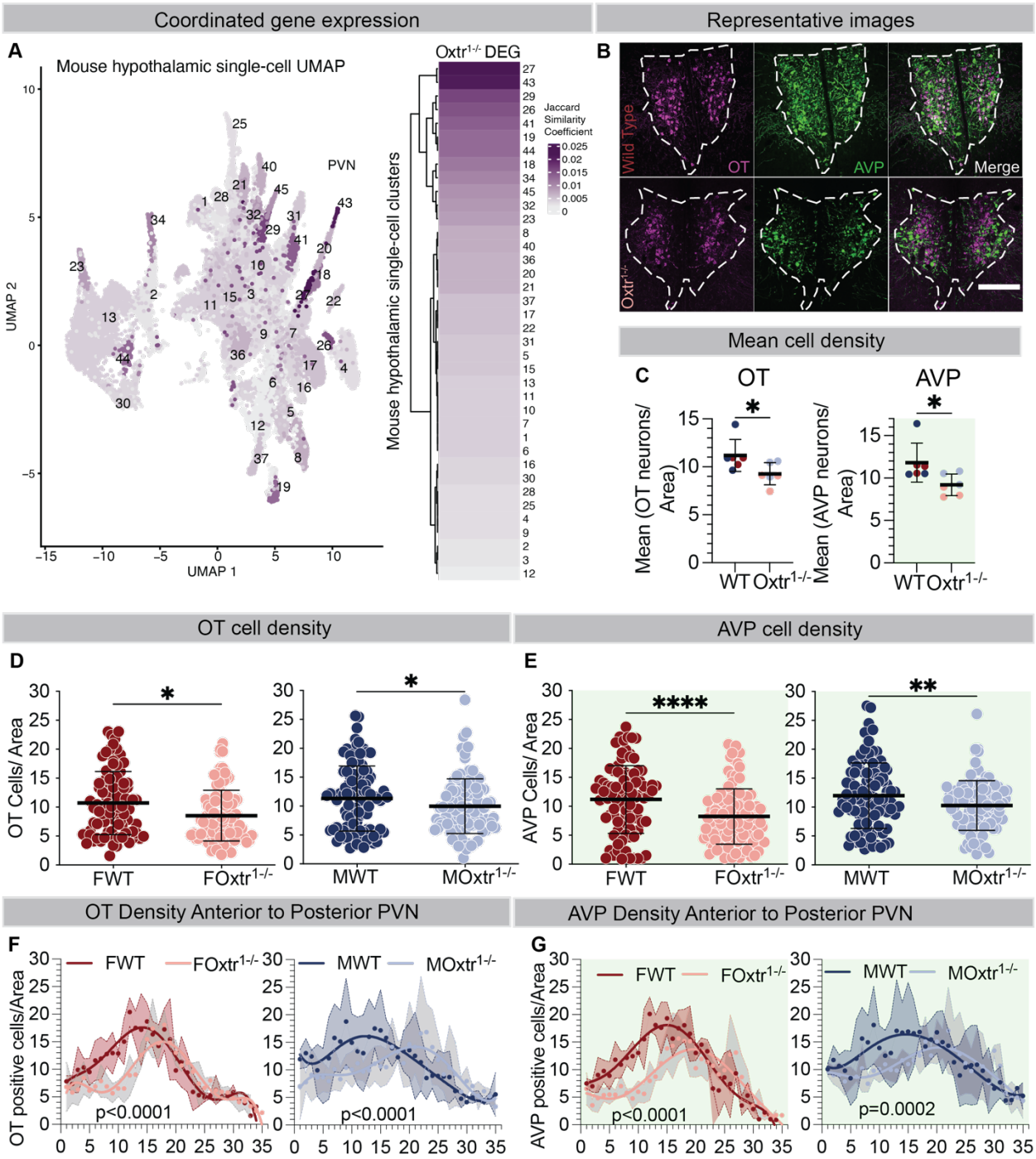

1294 **Figure7: Loss of Oxtr results in the decrease in density of Oxt and Avp**
1295 **expressing neurons in the PVN**

1296 A. UMAP visualization of mouse hypothalamus single-cell RNAseq dataset[83] with
1297 proposed PVN clusters labeled. The authors' original numeric cluster labels and
1298 embedding are shown. Each cluster is colored by the Jaccard similarity coefficient
1299 between the mouse marker gene sets and the vole Oxtr$^{1-/-}$ DE genes (ONP set).
1300 This is also represented in a heat plot to the right. Some of the highest similarity is
1301 seen in Cluster 43, which represents Oxt+ cells, and Cluster 26, which represents
1302 Avp+ cells in the PVN.

1303 B. Representative images of IHC staining against OT and AVP neuropeptides from
1304 FWT and FOxtr$^{1-/-}$ PVN showing the loss of structural integrity and OT and AVP
1305 positive cells from the knock-out. (White dotted line denotes the PVN area, scale
1306 bar represents 100μm)

1307 C. Mean of positive cells per unit area across all sections is lower for Oxtr$^{1-/-}$s vs WT
1308 for both OT (left) and AVP (right). Each dot represents 1 animal.

1309 D. The number of sections with a high density of OT positive cells is greater in both
1310 female (left) and male (right) WT animals.

1311 E. Similarly, WT animals of both sexes show an increase in the number of sections
1312 containing AVP positive neurons in high densities.

1313 F. The average OT cell density from matched PVN sections arranged from anterior
1314 to posterior shows that the decrease in cell density in Oxtr$^{1-/-}$ animals is biased
1315 towards the anterior. Each dot represents the average cell density, the lines

represent the sixth order non-linear regression model for cell density by sex and by genotype (n=3) and the ribbons represent the standard deviation.

G. $Oxtr^{1-/-}$ animals show a significant decrease in AVP cell density in the anterior PVN in both sexes.

See Supplementary Figure 7 and Supplementary Table 1.

Mean +/- SD, n = 3, *p =< 0.05, FWT = female WT, $FOxtr^{1-/-}$ = female $Oxtr^{1-/-}$, MWT = male WT, $MOxtr^{1-/-}$ = male $Oxtr^{1-/-}$.

References

1. Wilson, R.S., Krueger, K.R., Arnold, S.E., Schneider, J.A., Kelly, J.F., Barnes, L.L., Tang, Y., and Bennett, D.A. (2007). Loneliness and Risk of Alzheimer Disease. Arch Gen Psychiatry *64*, 234. https://doi.org/10.1001/archpsyc.64.2.234.

2. Bowlby, J., and Bowlby, J. (1982). Attachment 2. ed. (Basic Books).

3. Farinelli, M., Cevolani, D., Gestieri, L., Romaniello, C., Maffei, M., Agati, R., Leo, M.R., Huang, Z., Pedone, V., and Northoff, G. (2020). Brain and behaviour in post-acute stroke: Reduction in seeking and posterior cingulate neuronal variability. Journal of Clinical and Experimental Neuropsychology *42*, 584–601. https://doi.org/10.1080/13803395.2020.1780417.

4. Feldman, R., Monakhov, M., Pratt, M., and Ebstein, R.P. (2016). Oxytocin Pathway Genes: Evolutionary Ancient System Impacting on Human Affiliation, Sociality, and Psychopathology. Biological Psychiatry *79*, 174–184. https://doi.org/https://doi.org/10.1016/j.biopsych.2015.08.008.

5. Ebstein, R.P., Israel, S., Chew, S.H., Zhong, S., and Knafo, A. (2010). Genetics of human social behavior. Neuron *65*, 831–844. https://doi.org/10.1016/j.neuron.2010.02.020.

6. Winslow, J.T., Shapiro, L., Carter, C.S., and Insel, T.R. (1993). Oxytocin and complex social behavior: species comparisons. Psychopharmacol Bull *29*, 409–414.

7. Goodson, J.L. (2013). Deconstructing sociality, social evolution and relevant nonapeptide functions. Psychoneuroendocrinology *38*, 465–478. https://doi.org/10.1016/j.psyneuen.2012.12.005.

8. Harlow, H.F., and Harlow, M.K. (1965). THE EFFECT OF REARING CONDITIONS ON BEHAVIOR. Int J Psychiatry *1*, 43–51.

9. Shultz, S., Opie, C., and Atkinson, Q.D. (2011). Stepwise evolution of stable sociality in primates. Nature *479*, 219–222.

10. Insel, T.R., Winslow, J.T., Wang, Z., and Young, L.J. (1998). Oxytocin, vasopressin, and the neuroendocrine basis of pair bond formation. Adv. Exp. Med. Biol *449*, 215–224.

11. Klatt, J.D., and Goodson, J.L. (2013). Oxytocin-like receptors mediate pair bonding in a socially monogamous songbird. Proceedings of the Royal Society B: Biological Sciences *280*, 20122396. https://doi.org/10.1098/rspb.2012.2396.

12. Ainsworth, M.S. (1979). Infant–mother attachment. American Psychologist *34*, 932–937. https://doi.org/10.1037/0003-066X.34.10.932.

13. Getz, L.L., Carter, C.S., and Gavish, L. (1981). The mating system of the prairie vole, Microtus ochrogaster: Field and laboratory evidence for pair-bonding. Behav Ecol Sociobiol *8*, 189–194. https://doi.org/10.1007/BF00299829.

14. Donaldson, Z.R. (2010). We're the Same... but Different: Addressing Academic Divides in the Study of Brain and Behavior. Front Behav Neurosci *4*. https://doi.org/10.3389/fnbeh.2010.00041.

15. Insel, T.R., Winslow, J.T., Wang, Z.X., Young, L., and Hulihan, T.J. (1995). Oxytocin and the molecular basis of monogamy. Adv. Exp. Med. Biol *395*, 227–234.

16. Lukas, D., and Clutton-Brock, T.H. (2013). The evolution of social monogamy in mammals. Science *341*, 526–530.

17. Donaldson, Z.R., and Young, L.J. (2008). Oxytocin, vasopressin, and the neurogenetics of sociality. Science *322*, 900–904. https://doi.org/10.1126/science.1158668.

18. Bielsky, I.F., and Young, L.J. (2004). Oxytocin, vasopressin, and social recognition in mammals. Peptides *25*, 1565–1574. https://doi.org/10.1016/j.peptides.2004.05.019.

19. Nowicki, J.P., Pratchett, M.S., Walker, S.P.W., Coker, D.J., and O'Connell, L.A. (2020). Gene expression correlates of social evolution in coral reef butterflyfishes. Proceedings of the Royal Society B: Biological Sciences *287*, 20200239. https://doi.org/10.1098/rspb.2020.0239.

20. O'Connor, C.M., Marsh-Rollo, S.E., Aubin-Horth, N., and Balshine, S. (2016). Species-specific patterns of nonapeptide brain gene expression relative to pair-bonding behavior in

grouping and non-grouping cichlids. Hormones and Behavior *80*, 30–38. https://doi.org/10.1016/j.yhbeh.2015.10.015.

21. Stanley, D.A., and Adolphs, R. (2013). Toward a neural basis for social behavior. Neuron *80*, 816–826.

22. Insel, T.R. (1992). Oxytocin--a neuropeptide for affiliation: evidence from behavioral, receptor autoradiographic, and comparative studies. Psychoneuroendocrinology *17*, 3–35.

23. Lim, M.M., and Young, L.J. (2006). Neuropeptidergic regulation of affiliative behavior and social bonding in animals. Horm Behav *50*, 506–517. https://doi.org/10.1016/j.yhbeh.2006.06.028.

24. Carter, C.S., and Getz, L.L. (1993). Monogamy and the prairie vole. Sci. Am *268*, 100–106.

25. Beery, A.K., and Shambaugh, K.L. (2021). Comparative assessment of familiarity/novelty preferences in rodents. Frontiers in Behavioral Neuroscience *15*, 648830.

26. Beery, A.K., Christensen, J.D., Lee, N.S., and Blandino, K.L. (2018). Specificity in Sociality: Mice and Prairie Voles Exhibit Different Patterns of Peer Affiliation. Frontiers in Behavioral Neuroscience *12*, 50. https://doi.org/10.3389/fnbeh.2018.00050.

27. Schweinfurth, M.K., Neuenschwander, J., Engqvist, L., Schneeberger, K., Rentsch, A.K., Gygax, M., and Taborsky, M. (2017). Do female Norway rats form social bonds? Behavioral Ecology and Sociobiology *71*, 1–9.

28. Cho, M.M., DeVries, A.C., Williams, J.R., and Carter, C.S. (1999). The effects of oxytocin and vasopressin on partner preferences in male and female prairie voles (Microtus ochrogaster). Behav. Neurosci *113*, 1071–1079.

29. Insel, T.R., and Hulihan, T.J. (1995). A gender-specific mechanism for pair bonding: oxytocin and partner preference formation in monogamous voles. Behav. Neurosci *109*, 782–789.

30. Williams, J.R., Catania, K.C., and Carter, C.S. (1992). Development of partner preferences in female prairie voles (Microtus ochrogaster): the role of social and sexual experience. Hormones and behavior *26*, 339–349.

31. Wang, Z., Hulihan, T.J., and Insel, T.R. (1997). Sexual and social experience is associated with different patterns of behavior and neural activation in male prairie voles. Brain Res *767*, 321–332.

32. Xu, X., Coats, J.K., Yang, C.F., Wang, A., Ahmed, O.M., Alvarado, M., Izumi, T., and Shah, N.M. (2012). Modular genetic control of sexually dimorphic behaviors. Cell *148*, 596–607. https://doi.org/10.1016/j.cell.2011.12.018.

1411 33. Villella, A., and Hall, J.C. (2008). Chapter 3 Neurogenetics of Courtship and Mating in
1412 Drosophila. In Advances in Genetics (Elsevier), pp. 67–184. https://doi.org/10.1016/S0065-
1413 2660(08)00603-2.

1414 34. Konopka, R.J., and Benzer, S. (1971). Clock Mutants of *Drosophila melanogaster*. Proc Natl
1415 Acad Sci USA *68*, 2112–2116. https://doi.org/10.1073/pnas.68.9.2112.

1416 35. Takahashi, J.S., Shimomura, K., and Kumar, V. (2008). Searching for genes underlying
1417 behavior: lessons from circadian rhythms. Science *322*, 909–912.
1418 https://doi.org/10.1126/science.1158822.

1419 36. Baker, B.S., Taylor, B.J., and Hall, J.C. (2001). Are complex behaviors specified by
1420 dedicated regulatory genes? Reasoning from Drosophila. Cell *105*, 13–24.

1421 37. Manoli, D.S., and Baker, B.S. (2004). Median bundle neurons coordinate behaviours during
1422 Drosophila male courtship. Nature *430*, 564–569. https://doi.org/10.1038/nature02713.

1423 38. Martin, L.B., Glasper, E.R., Nelson, R.J., and DeVries, A.C. (2006). Prolonged separation
1424 delays wound healing in monogamous California mice, Peromyscus californicus, but not in
1425 polygynous white-footed mice, P. leucopus. Physiology & Behavior *87*, 837–841.
1426 https://doi.org/10.1016/j.physbeh.2006.01.035.

1427 39. Ferland, C.L., and Schrader, L.A. (2011). Cage mate separation in pair-housed male rats
1428 evokes an acute stress corticosterone response. Neuroscience Letters *489*, 154–158.
1429 https://doi.org/10.1016/j.neulet.2010.12.006.

1430 40. Okuda, T., Osako, Y., Hidaka, C., Nishihara, M., Young, L.J., Mitsui, S., and Yuri, K. (2022).
1431 Separation from a bonded partner alters neural response to inflammatory pain in
1432 monogamous rodents. Behavioural Brain Research *418*, 113650.
1433 https://doi.org/10.1016/j.bbr.2021.113650.

1434 41. Carter, C.S., Williams, J.R., Witt, D.M., and Insel, T.R. (1992). Oxytocin and social bonding.
1435 Ann. N. Y. Acad. Sci *652*, 204–211.

1436 42. Winslow, J.T., Hastings, N., Carter, C.S., Harbaugh, C.R., and Insel, T.R. (1993). A role for
1437 central vasopressin in pair bonding in monogamous prairie voles. Nature *365*, 545–548.
1438 https://doi.org/10.1038/365545a0.

1439 43. Carter, C.S., Grippo, A.J., Pournajafi-Nazarloo, H., Ruscio, M.G., and Porges, S.W. (2008).
1440 Oxytocin, vasopressin and sociality. Prog. Brain Res *170*, 331–336.
1441 https://doi.org/10.1016/S0079-6123(08)00427-5.

1442 44. Ophir, A.G., Gessel, A., Zheng, D.-J., and Phelps, S.M. (2012). Oxytocin receptor density is
1443 associated with male mating tactics and social monogamy. Hormones and behavior *61*, 445–
1444 453.

1445 45. Shapiro, L.E., and Insel, T.R. (1992). Oxytocin receptor distribution reflects social
1446 organization in monogamous and polygamous voles. Ann. N. Y. Acad. Sci *652*, 448–451.

46. Heinrichs, M., von Dawans, B., and Domes, G. (2009). Oxytocin, vasopressin, and human social behavior. Front Neuroendocrinol *30*, 548–557. https://doi.org/10.1016/j.yfrne.2009.05.005.

47. Insel, T.R., Wang, Z.X., and Ferris, C.F. (1994). Patterns of brain vasopressin receptor distribution associated with social organization in microtine rodents. J. Neurosci *14*, 5381–5392.

48. King, L.B., Walum, H., Inoue, K., Eyrich, N.W., and Young, L.J. (2016). Variation in the oxytocin receptor gene predicts brain region–specific expression and social attachment. Biological psychiatry *80*, 160–169.

49. Walum, H., and Young, L.J. (2018). The neural mechanisms and circuitry of the pair bond. Nat Rev Neurosci *19*, 643–654. https://doi.org/10.1038/s41583-018-0072-6.

50. Williams, J.R., Insel, T.R., Harbaugh, C.R., and Carter, C.S. (1994). Oxytocin administered centrally facilitates formation of a partner preference in female prairie voles (Microtus ochrogaster). J. Neuroendocrinol *6*, 247–250.

51. Bales, K.L., and Carter, C.S. (2003). Developmental exposure to oxytocin facilitates partner preferences in male prairie voles (Microtus ochrogaster). Behavioral neuroscience *117*, 854.

52. Keebaugh, A.C., and Young, L.J. (2011). Increasing oxytocin receptor expression in the nucleus accumbens of pre-pubertal female prairie voles enhances alloparental responsiveness and partner preference formation as adults. Hormones and Behavior *60*, 498–504. https://doi.org/https://doi.org/10.1016/j.yhbeh.2011.07.018.

53. Romero, T., Nagasawa, M., Mogi, K., Hasegawa, T., and Kikusui, T. (2014). Oxytocin promotes social bonding in dogs. Proc Natl Acad Sci U S A *111*, 9085–9090. https://doi.org/10.1073/pnas.1322868111.

54. Nagasawa, M., Mitsui, S., En, S., Ohtani, N., Ohta, M., Sakuma, Y., Onaka, T., Mogi, K., and Kikusui, T. (2015). Social evolution. Oxytocin-gaze positive loop and the coevolution of human-dog bonds. Science *348*, 333–336. https://doi.org/10.1126/science.1261022.

55. Smith, A.S., Agmo, A., Birnie, A.K., and French, J.A. (2010). Manipulation of the oxytocin system alters social behavior and attraction in pair-bonding primates, Callithrix penicillata. Horm Behav *57*, 255–262. https://doi.org/10.1016/j.yhbeh.2009.12.004.

56. Duque, J.F., Leichner, W., Ahmann, H., and Stevens, J.R. (2018). Mesotocin influences pinyon jay prosociality. Biol Lett *14*. https://doi.org/10.1098/rsbl.2018.0105.

57. Oldfield, R.G., and Hofmann, H.A. (2011). Neuropeptide regulation of social behavior in a monogamous cichlid fish. Physiology & Behavior *102*, 296–303. https://doi.org/https://doi.org/10.1016/j.physbeh.2010.11.022.

58. Klatt, J.D., and Goodson, J.L. (2013). Oxytocin-like receptors mediate pair bonding in a socially monogamous songbird. Proc Biol Sci *280*, 20122396. https://doi.org/10.1098/rspb.2012.2396.

59. Berendzen, K.M., Sharma, R., Mandujano, M.A., Wei, Y., Rogers, F.D., Simmons, T.C., Seelke, A.M., Bond, J.M., Larios, R., Goodwin, N.L., et al. (2023). Oxytocin receptor is not required for social attachment in prairie voles. Neuron *111*, 787–796.

60. Young, L.J., Lim, M.M., Gingrich, B., and Insel, T.R. (2001). Cellular mechanisms of social attachment. Hormones and behavior *40*, 133–138.

61. Tripp, J.A., Berrio, A., McGraw, L.A., Matz, M.V., Davis, J.K., Inoue, K., Thomas, J.W., Young, L.J., and Phelps, S.M. (2021). Comparative neurotranscriptomics reveal widespread species differences associated with bonding. BMC Genomics *22*, 399. https://doi.org/10.1186/s12864-021-07720-0.

62. Grinevich, V., DesarmÃ©nien, M.G., Chini, B., Tauber, M., and Muscatelli, F. (2015). Ontogenesis of oxytocin pathways in the mammalian brain: late maturation and psychosocial disorders. Front. Neuroanat. *8*. https://doi.org/10.3389/fnana.2014.00164.

63. Newmaster, K.T., Nolan, Z.T., Chon, U., Vanselow, D.J., Weit, A.R., Tabbaa, M., Hidema, S., Nishimori, K., Hammock, E.A.D., and Kim, Y. (2020). Quantitative cellular-resolution map of the oxytocin receptor in postnatally developing mouse brains. Nature Communications *11*, 1885. https://doi.org/10.1038/s41467-020-15659-1.

64. Yamamoto, Y., Cushing, B.S., Kramer, K.M., Epperson, P.D., Hoffman, G.E., and Carter, C.S. (2004). Neonatal manipulations of oxytocin alter expression of oxytocin and vasopressin immunoreactive cells in the paraventricular nucleus of the hypothalamus in a gender-specific manner. Neuroscience *125*, 947–955. https://doi.org/10.1016/j.neuroscience.2004.02.028.

65. Mitre, M., Saadipour, K., Williams, K., Khatri, L., Froemke, R.C., and Chao, M.V. (2022). Transactivation of TrkB Receptors by Oxytocin and Its G Protein-Coupled Receptor. Front Mol Neurosci *15*, 891537. https://doi.org/10.3389/fnmol.2022.891537.

66. Young, L.J., and Wang, Z. (2004). The neurobiology of pair bonding. Nat. Neurosci *7*, 1048–1054. https://doi.org/10.1038/nn1327.

67. DeVries, A.C., and Carter, C.S. (1999). Sex differences in temporal parameters of partner preference in prairie voles (Microtus ochrogaster). Can. J. Zool. *77*, 885–889. https://doi.org/10.1139/z99-054.

68. Fraser, E.J., and Shah, N.M. (2014). Complex Chemosensory Control of Female Reproductive Behaviors. PLOS ONE *9*, e90368. https://doi.org/10.1371/journal.pone.0090368.

69. Aragona, B.J., Liu, Y., Curtis, J.T., Stephan, F.K., and Wang, Z. (2003). A Critical Role for Nucleus Accumbens Dopamine in Partner-Preference Formation in Male Prairie Voles. J. Neurosci. *23*, 3483–3490. https://doi.org/10.1523/JNEUROSCI.23-08-03483.2003.

70. Dölen, G., Darvishzadeh, A., Huang, K.W., and Malenka, R.C. (2013). Social reward requires coordinated activity of nucleus accumbens oxytocin and serotonin. Nature *501*, 179–184. https://doi.org/10.1038/nature12518.

71. Ross, H.E., Freeman, S.M., Spiegel, L.L., Ren, X., Terwilliger, E.F., and Young, L.J. (2009). Variation in Oxytocin Receptor Density in the Nucleus Accumbens Has Differential Effects on Affiliative Behaviors in Monogamous and Polygamous Voles. J. Neurosci. *29*, 1312–1318. https://doi.org/10.1523/JNEUROSCI.5039-08.2009.

72. Langfelder, P., and Horvath, S. (2008). WGCNA: an R package for weighted correlation network analysis. BMC Bioinformatics *9*, 559. https://doi.org/10.1186/1471-2105-9-559.

73. Maury, E.A., Sherman, M.A., Genovese, G., Gilgenast, T.G., Kamath, T., Burris, S.J., Rajarajan, P., Flaherty, E., Akbarian, S., Chess, A., et al. (2023). Schizophrenia-associated somatic copy-number variants from 12,834 cases reveal recurrent NRXN1 and ABCB11 disruptions. Cell Genom *3*, 100356. https://doi.org/10.1016/j.xgen.2023.100356.

74. Satterstrom, F.K., Kosmicki, J.A., Wang, J., Breen, M.S., De Rubeis, S., An, J.-Y., Peng, M., Collins, R., Grove, J., Klei, L., et al. (2020). Large-Scale Exome Sequencing Study Implicates Both Developmental and Functional Changes in the Neurobiology of Autism. Cell *180*, 568-584.e23. https://doi.org/10.1016/j.cell.2019.12.036.

75. Fromer, M., Pocklington, A.J., Kavanagh, D.H., Williams, H.J., Dwyer, S., Gormley, P., Georgieva, L., Rees, E., Palta, P., Ruderfer, D.M., et al. (2014). De novo mutations in schizophrenia implicate synaptic networks. Nature *506*, 179–184. https://doi.org/10.1038/nature12929.

76. EuroEPINOMICS-RES Consortium, Epilepsy Phenome/Genome Project, and Epi4K Consortium (2014). De novo mutations in synaptic transmission genes including DNM1 cause epileptic encephalopathies. Am J Hum Genet *95*, 360–370. https://doi.org/10.1016/j.ajhg.2014.08.013.

77. Kaplanis, J., Samocha, K.E., Wiel, L., Zhang, Z., Arvai, K.J., Eberhardt, R.Y., Gallone, G., Lelieveld, S.H., Martin, H.C., McRae, J.F., et al. (2020). Evidence for 28 genetic disorders discovered by combining healthcare and research data. Nature *586*, 757–762. https://doi.org/10.1038/s41586-020-2832-5.

78. Inoue, K., Ford, C.L., Horie, K., and Young, L.J. (2022). Oxytocin receptors are widely distributed in the prairie vole (Microtus ochrogaster) brain: Relation to social behavior, genetic polymorphisms, and the dopamine system. J Comp Neurol *530*, 2881–2900. https://doi.org/10.1002/cne.25382.

79. Lefevre, A., Benusiglio, D., Tang, Y., Krabichler, Q., Charlet, A., and Grinevich, V. (2021). Oxytocinergic Feedback Circuitries: An Anatomical Basis for Neuromodulation of Social Behaviors. Front. Neural Circuits *15*, 688234. https://doi.org/10.3389/fncir.2021.688234.

80. Harris, G.W. (1955). PITUITARY-HYPOTHALAMIC MECHANISMS. Arch NeurPsych *73*, 124. https://doi.org/10.1001/archneurpsyc.1955.02330080002002.

81. Ye, Q., Nunez, J., and Zhang, X. (2022). Oxytocin Receptor-Expressing Neurons in the Paraventricular Thalamus Regulate Feeding Motivation through Excitatory Projections to the Nucleus Accumbens Core. J. Neurosci. *42*, 3949–3964. https://doi.org/10.1523/JNEUROSCI.2042-21.2022.

82. Zhang, B., Qiu, L., Xiao, W., Ni, H., Chen, L., Wang, F., Mai, W., Wu, J., Bao, A., Hu, H., et al. (2021). Reconstruction of the Hypothalamo-Neurohypophysial System and Functional Dissection of Magnocellular Oxytocin Neurons in the Brain. Neuron *109*, 331-346.e7. https://doi.org/10.1016/j.neuron.2020.10.032.

83. Romanov, R.A., Tretiakov, E.O., Kastriti, M.E., Zupancic, M., Häring, M., Korchynska, S., Popadin, K., Benevento, M., Rebernik, P., Lallemend, F., et al. (2020). Molecular design of hypothalamus development. Nature *582*, 246–252. https://doi.org/10.1038/s41586-020-2266-0.

84. Seoyoung Son, Steffy B. Manjila, Kyra T. Newmaster, Yuan-ting Wu, Daniel J. Vanselow, Matt Ciarletta, Todd E. Anthony, Keith C. Cheng, and Yongsoo Kim (2022). Whole-Brain Wiring Diagram of Oxytocin System in Adult Mice. J. Neurosci. *42*, 5021. https://doi.org/10.1523/JNEUROSCI.0307-22.2022.

85. Vaidyanathan, R., and Hammock, E.A.D. (2020). Oxytocin receptor gene loss influences expression of the oxytocin gene in C57BL/6J mice in a sex- and age-dependent manner. Journal of Neuroendocrinology *32*, e12821. https://doi.org/10.1111/jne.12821.

86. Kleiman, D.G. (1977). Monogamy in Mammals. The Quarterly Review of Biology *52*, 39–69. https://doi.org/10.1086/409721.

87. Feldman, R. (2017). The Neurobiology of Human Attachments. Trends in Cognitive Sciences *21*, 80–99. https://doi.org/10.1016/j.tics.2016.11.007.

88. Johnson, Z.V., Walum, H., Jamal, Y.A., Xiao, Y., Keebaugh, A.C., Inoue, K., and Young, L.J. (2016). Central oxytocin receptors mediate mating-induced partner preferences and enhance correlated activation across forebrain nuclei in male prairie voles. Horm Behav *79*, 8–17. https://doi.org/10.1016/j.yhbeh.2015.11.011.

89. Takayanagi, Y., Yoshida, M., Bielsky, I.F., Ross, H.E., Kawamata, M., Onaka, T., Yanagisawa, T., Kimura, T., Matzuk, M.M., Young, L.J., et al. (2005). Pervasive social deficits, but normal parturition, in oxytocin receptor-deficient mice. PNAS *102*, 16096–16101.

90. Pobbe, R.L.H., Pearson, B.L., Defensor, E.B., Bolivar, V.J., Young, W.S., Lee, H.-J., Blanchard, D.C., and Blanchard, R.J. (2012). Oxytocin receptor knockout mice display deficits in the expression of autism-related behaviors. Hormones and Behavior *61*, 436–444. https://doi.org/https://doi.org/10.1016/j.yhbeh.2011.10.010.

91. Yang, C.F., and Shah, N.M. (2014). Representing sex in the brain, one module at a time. Neuron *82*, 261–278. https://doi.org/10.1016/j.neuron.2014.03.029.

92. Mong, J.A., and Pfaff, D.W. (2004). Hormonal symphony: steroid orchestration of gene modules for sociosexual behaviors. Mol Psychiatry *9*, 550–556. https://doi.org/10.1038/sj.mp.4001493.

93. Mong, J., Easton, A., Kow, L.M., and Pfaff, D. (2003). Neural, hormonal and genetic mechanisms for the activation of brain and behavior. Eur J Pharmacol *480*, 229–231. https://doi.org/10.1016/j.ejphar.2003.08.109.

94. Barron, A.B., and Robinson, G.E. (2008). The utility of behavioral models and modules in molecular analyses of social behavior. Genes Brain and Behavior *7*, 257–265. https://doi.org/10.1111/j.1601-183X.2007.00344.x.

95. Kyriacou, C.P., and Hall, J.C. (1980). Circadian rhythm mutations in Drosophila melanogaster affect short-term fluctuations in the male's courtship song. Proc Natl Acad Sci U S A *77*, 6729–6733. https://doi.org/10.1073/pnas.77.11.6729.

96. Konopka, R.J., and Benzer, S. (1971). Clock Mutants of *Drosophila melanogaster*. Proc Natl Acad Sci USA *68*, 2112–2116. https://doi.org/10.1073/pnas.68.9.2112.

97. Bendesky, A., Kwon, Y.-M., Lassance, J.-M., Lewarch, C.L., Yao, S., Peterson, B.K., He, M.X., Dulac, C., and Hoekstra, H.E. (2017). The genetic basis of parental care evolution in monogamous mice. Nature *544*, 434–439. https://doi.org/10.1038/nature22074.

98. Scheele, D., Striepens, N., Güntürkün, O., Deutschländer, S., Maier, W., Kendrick, K.M., and Hurlemann, R. (2012). Oxytocin modulates social distance between males and females. J Neurosci *32*, 16074–16079. https://doi.org/10.1523/JNEUROSCI.2755-12.2012.

99. Ditzen, B., Schaer, M., Gabriel, B., Bodenmann, G., Ehlert, U., and Heinrichs, M. (2009). Intranasal Oxytocin Increases Positive Communication and Reduces Cortisol Levels During Couple Conflict. Biological Psychiatry *65*, 728–731. https://doi.org/10.1016/j.biopsych.2008.10.011.

100. De Dreu, C.K.W., Greer, L.L., Handgraaf, M.J.J., Shalvi, S., Van Kleef, G.A., Baas, M., Ten Velden, F.S., Van Dijk, E., and Feith, S.W.W. (2010). The Neuropeptide Oxytocin Regulates Parochial Altruism in Intergroup Conflict Among Humans. Science *328*, 1408–1411. https://doi.org/10.1126/science.1189047.

101. Osakada, T., Yan, R., Jiang, Y., Wei, D., Tabuchi, R., Dai, B., Wang, X., Zhao, G., Wang, C.X., Liu, J.-J., et al. (2024). A dedicated hypothalamic oxytocin circuit controls aversive social learning. Nature *626*, 347–356. https://doi.org/10.1038/s41586-023-06958-w.

1625 102. Wang, Z., and Young, L.J. (1997). Ontogeny of oxytocin and vasopressin receptor
1626 binding in the lateral septum in prairie and montane voles. Brain Res. Dev. Brain Res *104*,
1627 191–195.

1628 103. Smith, M.L., Asada, N., and Malenka, R.C. (2021). Anterior cingulate inputs to nucleus
1629 accumbens control the social transfer of pain and analgesia. Science *371*, 153–159.
1630 https://doi.org/10.1126/science.abe3040.

1631 104. Gegenhuber, B., Wu, M.V., Bronstein, R., and Tollkuhn, J. (2020). Regulation of neural
1632 gene expression by estrogen receptor alpha (Neuroscience)
1633 https://doi.org/10.1101/2020.10.21.349290.

1634 105. Cao, J., and Patisaul, H.B. (2013). Sex-specific expression of estrogen receptors α and β
1635 and Kiss1 in the postnatal rat amygdala. J of Comparative Neurology *521*, 465–478.
1636 https://doi.org/10.1002/cne.23185.

1637 106. Mitsushima, D., Yamada, K., Takase, K., Funabashi, T., and Kimura, F. (2006). Sex
1638 differences in the basolateral amygdala: the extracellular levels of serotonin and dopamine,
1639 and their responses to restraint stress in rats. Eur J Neurosci *24*, 3245–3254.
1640 https://doi.org/10.1111/j.1460-9568.2006.05214.x.

1641 107. McCann, K.E., Sinkiewicz, D.M., Rosenhauer, A.M., Beach, L.Q., and Huhman, K.L.
1642 (2019). Transcriptomic Analysis Reveals Sex-Dependent Expression Patterns in the
1643 Basolateral Amygdala of Dominant and Subordinate Animals After Acute Social Conflict.
1644 Mol Neurobiol *56*, 3768–3779. https://doi.org/10.1007/s12035-018-1339-7.

1645 108. Trainor, B.C. (2011). Stress responses and the mesolimbic dopamine system: social
1646 contexts and sex differences. Horm Behav *60*, 457–469.
1647 https://doi.org/10.1016/j.yhbeh.2011.08.013.

1648 109. Wright, E.C., Luo, P.X., Zakharenkov, H.C., Serna Godoy, A., Lake, A.A., Prince, Z.D.,
1649 Sekar, S., Culkin, H.I., Ramirez, A.V., Dwyer, T., et al. (2023). Sexual differentiation of
1650 neural mechanisms of stress sensitivity during puberty. Proc. Natl. Acad. Sci. U.S.A. *120*,
1651 e2306475120. https://doi.org/10.1073/pnas.2306475120.

1652 110. Dölen, G. (2015). Oxytocin: parallel processing in the social brain? J. Neuroendocrinol.
1653 *27*, 516–535. https://doi.org/10.1111/jne.12284.

1654 111. Choi, T.-Y., Jeon, H., Jeong, S., Kim, E.J., Kim, J., Jeong, Y.H., Kang, B., Choi, M., and
1655 Koo, J.W. (2023). Distinct prefrontal projection activity and transcriptional state conversely
1656 orchestrate social competition and hierarchy. Neuron, S0896-6273(23)00886-3.
1657 https://doi.org/10.1016/j.neuron.2023.11.012.

1658 112. Yaguchi, K., Hagihara, M., Konno, A., Hirai, H., Yukinaga, H., and Miyamichi, K.
1659 (2023). Dynamic modulation of pulsatile activities of oxytocin neurons in lactating wild-type
1660 mice. PLoS One *18*, e0285589. https://doi.org/10.1371/journal.pone.0285589.

113. Newmaster, K.T., Nolan, Z.T., Chon, U., Vanselow, D.J., Weit, A.R., Tabbaa, M., Hidema, S., Nishimori, K., Hammock, E.A.D., and Kim, Y. (2020). Quantitative cellular-resolution map of the oxytocin receptor in postnatally developing mouse brains. Nat Commun *11*, 1885. https://doi.org/10.1038/s41467-020-15659-1.

114. Vaidyanathan, R., and Hammock, E.A.D. (2017). Oxytocin receptor dynamics in the brain across development and species. Developmental Neurobiology *77*, 143–157. https://doi.org/10.1002/dneu.22403.

115. Manoli, D.S., and State, M.W. (2021). Autism Spectrum Disorder Genetics and the Search for Pathological Mechanisms. AJP *178*, 30–38. https://doi.org/10.1176/appi.ajp.2020.20111608.

116. Werling, D.M. (2016). The role of sex-differential biology in risk for autism spectrum disorder. Biology of Sex Differences *7*, 58. https://doi.org/10.1186/s13293-016-0112-8.

117. Werling, D.M., and Geschwind, D.H. (2013). Sex differences in autism spectrum disorders. Curr. Opin. Neurol. *26*, 146–153. https://doi.org/10.1097/WCO.0b013e32835ee548.

118. Perissi, V., and Rosenfeld, M.G. (2005). Controlling nuclear receptors: the circular logic of cofactor cycles. Nature Reviews: Molecular Cell Biology *6*, 542–554. https://doi.org/10.1038/nrm1682.

119. Horie, K., Inoue, K., Nishimori, K., and Young, L.J. (2020). Investigation of Oxtr-expressing Neurons Projecting to Nucleus Accumbens using Oxtr-ires-Cre Knock-in prairie Voles (Microtus ochrogaster). Neuroscience *448*, 312–324. https://doi.org/10.1016/j.neuroscience.2020.08.023.

120. Villanueva, C., Jacquier, S., and de Roux, N. (2012). DLK1 Is a Somato-Dendritic Protein Expressed in Hypothalamic Arginine-Vasopressin and Oxytocin Neurons. PLoS One *7*, e36134. https://doi.org/10.1371/journal.pone.0036134.

121. Insel, T.R. (1997). A neurobiological basis of social attachment. Am J Psychiatry *154*, 726–735.

122. Carter, C.S., and Perkeybile, A.M. (2018). The Monogamy Paradox: What Do Love and Sex Have to Do With It? Front. Ecol. Evol. *6*, 202. https://doi.org/10.3389/fevo.2018.00202.

123. De Vries, G.J. (2004). Minireview: Sex Differences in Adult and Developing Brains: Compensation, Compensation, Compensation. Endocrinology *145*, 1063–1068. https://doi.org/10.1210/en.2003-1504.

124. Friard, O., and Gamba, M. (2016). BORIS: a free, versatile open-source event-logging software for video/audio coding and live observations. Methods in ecology and evolution *7*, 1325–1330.

125. Risso, D., Ngai, J., Speed, T.P., and Dudoit, S. (2014). Normalization of RNA-seq data using factor analysis of control genes or samples. Nat Biotechnol *32*, 896–902. https://doi.org/10.1038/nbt.2931.

126. Love, M.I., Huber, W., and Anders, S. (2014). Moderated estimation of fold change and dispersion for RNA-seq data with DESeq2. Genome Biol *15*, 550. https://doi.org/10.1186/s13059-014-0550-8.

127. Stephens, M., Carbonetto, P., Gerard, D., Lu, M., Sun, L., Willwerscheid, J., and Xiao, N. (2020). Methods for Adaptive Shrinkage, using Empirical Bayes [R package ashr version 2.2-47]. In.

128. Young, M.D., Wakefield, M.J., Smyth, G.K., and Oshlack, A. (2010). Gene ontology analysis for RNA-seq: accounting for selection bias. Genome Biol *11*, R14. https://doi.org/10.1186/gb-2010-11-2-r14.

129. Yu, G. (2020). Gene Ontology Semantic Similarity Analysis Using GOSemSim. In Stem Cell Transcriptional Networks Methods in Molecular Biology., B. L. Kidder, ed. (Springer US), pp. 207–215. https://doi.org/10.1007/978-1-0716-0301-7_11.

130. Pico, A.R., Kelder, T., Van Iersel, M.P., Hanspers, K., Conklin, B.R., and Evelo, C. (2008). WikiPathways: Pathway Editing for the People. PLoS Biol *6*, e184. https://doi.org/10.1371/journal.pbio.0060184.

131. Wu, T., Hu, E., Xu, S., Chen, M., Guo, P., Dai, Z., Feng, T., Zhou, L., Tang, W., Zhan, L., et al. (2021). clusterProfiler 4.0: A universal enrichment tool for interpreting omics data. The Innovation *2*, 100141. https://doi.org/10.1016/j.xinn.2021.100141.

132. Fu, R., Gillen, A.E., Sheridan, R.M., Tian, C., Daya, M., Hao, Y., Hesselberth, J.R., and Riemondy, K.A. (2020). clustifyr: an R package for automated single-cell RNA sequencing cluster classification. F1000Res *9*, 223. https://doi.org/10.12688/f1000research.22969.2.

133. Zhang, B., and Horvath, S. (2005). A general framework for weighted gene co-expression network analysis. Stat Appl Genet Mol Biol *4*, Article17. https://doi.org/10.2202/1544-6115.1128.

134. Langfelder, P., Luo, R., Oldham, M.C., and Horvath, S. (2011). Is my network module preserved and reproducible? PLoS Comput Biol *7*, e1001057. https://doi.org/10.1371/journal.pcbi.1001057.

135. Gandrillon, O., Solari, F., Legrand, C., Jurdic, P., and Samarut, J. (1996). A rapid and convenient method to prepare DIG-labelled RNA probes for use in non-radioactive in situ hybridization. Molecular and cellular probes *10*, 51–56.